

## INITIAL-VALUE PROBLEMS IN TWO AND THREE DIMENSIONS

### 10-1 CLASSICAL INITIAL-VALUE PROBLEMS IN TIME

It is easiest to cover fundamentals with the heat-flow equation in one dimension. The heat-flow equation is derived from two intuitively obvious equations. The first says that a flow  $H$  of heat arises from a temperature gradient and is proportional to thermal conductivity  $\sigma$ .

$$H = -\sigma \frac{\partial T}{\partial x} \quad (10-1-1)$$

The second says the temperature decrease is in proportion to the divergence of heat flow  $H$  and inversely proportional to the heat capacity  $C$  of the material

$$\frac{\partial T}{\partial t} = -\frac{1}{C} \frac{\partial H}{\partial x} \quad (10-1-2)$$

The usual procedure is to insert (10-1-1) into (10-1-2) and neglect the derivative of  $\sigma$ .

$$\frac{\partial T}{\partial t} = \frac{\sigma}{C} \frac{\partial^2 T}{\partial x^2} \quad (10-1-3)$$

The usual convention in difference equation theory is that temperature  $T(x, t) = T(k \Delta x, n \Delta t)$  will be written as  $T_k^n$  where the superscript denotes time. With the definition  $b = \sigma \Delta t / 2C \Delta x^2$  (10-1-3) may be written

$$T_k^{n+1} - T_k^n = 2b(T_{k+1}^n - 2T_k^n + T_{k-1}^n) \quad (10-1-4)$$

If the temperature  $T_k^n$  is known at all spatial positions  $k$  for some particular time  $n$ , then (10-1-4) may be used to calculate the temperature for all time. The reader may notice that the time derivative is centered at  $T_k^{n+1/2}$  whereas the space derivative is centered at  $T_k^n$ . This can cause difficulty. The heat-flow differential equation smooths out long spatial wavelengths slowly and shorter wavelengths more rapidly. The heat-flow difference equation does the same thing, except that very short wavelengths will sense the difference in centering of time and space derivatives. The result is that the very short wavelengths will not attenuate at the proper rate and they may even amplify. In fact, as  $\Delta x$  is reduced more and more, thereby making it possible to contain shorter and shorter wavelengths on the grid, amplification will always occur, thereby ruining the solution. This situation, called instability, is described in more detail in all the books on the subject. One might hope that centering the time difference by approximating  $\partial T / \partial t$  by  $(T_k^{n+1} - T_k^{n-1}) / (2\Delta t)$  would avoid the instability, but it turns out even worse and creates instability for any  $\Delta x$ . The reason is that the heat-flow differential equation is first-order in time, but using a time difference over two steps creates a difference equation which is second-order in time. A second-order equation always has two solutions. In this case, one behaves like the heat-flow equation; the other turns out to be an oscillating increasing exponential like  $(1, -2, 4, -8, \dots)$  which rapidly overwhelms the heat-flow solution.

These problems may all be avoided with the Crank-Nicolson scheme. It will always guarantee stability for any  $\Delta x$  and it can also be applied to the wave equations

There are whole textbooks (for example, References 33 and 34) devoted to solving initial-value problems by difference approximations to differential equations. In this section we will briefly cover the main ideas. The overall idea in two dimensions is that one partitions a computer memory into one or a few two-dimensional grids where field variables are represented as functions of two spatial dimensions. Then you insert initial conditions, turn on the computer, and see what happens. There have been numerous extensive studies devoted to the diffusion equation, but far fewer studies have been devoted to the wave equation. The problem with modeling the wave equation is that ten points per wavelength is probably not enough, and even at that you cannot fit very many wavelengths onto a reasonable grid. The energy then propagates rapidly to the edges of the grid where it bounces back, whether you want it to or not. One way to ameliorate this kind of difficulty is to develop coordinate systems which move with the waves. These coordinate systems also facilitate projection of waves from the earth's surface, where they are observed, back down into the earth. This kind of projection forms the basis for the practical reflection seismic data processing techniques described in chapter 11.

in acoustics, electromagnetics, and elasticity. In the Crank-Nicolson scheme one centers the space difference at  $T_k^{n+1/2}$  in the following way:

$$T_k^{n+1} - T_k^n = b(T_{k+1}^n - 2T_k^n + T_{k-1}^n) + b(T_{k+1}^{n+1} - 2T_k^{n+1} + T_{k-1}^{n+1}) \quad (10-1-5)$$

An apparent problem with the Crank-Nicolson scheme is that the method of getting the  $n+1$  time level from the  $n$  level is no longer obvious. Bringing all the  $n+1$  terms in (10-1-5) to the left and the  $n$  terms to the right, we have

$$-bT_{k+1}^{n+1} + (1+2b)T_k^{n+1} - bT_{k-1}^{n+1} = D_k^n \quad (10-1-6)$$

The right-hand side  $D_k^n$  is a known function of  $T^n$ . What we have here is a set of simultaneous equations for the  $T^{n+1}$ . Writing this out in full, we see why the set is called a tridiagonal set of equations

$$\begin{bmatrix} (1+2b) & -b & & & \text{zeros} \\ -b & (1+2b) & -b & & \\ & -b & (1+2b) & -b & \\ & & & & \\ \text{zeros} & & & & \end{bmatrix} \begin{bmatrix} T_0^{n+1} \\ T_1^{n+1} \\ \vdots \\ T_N^{n+1} \end{bmatrix} = \begin{bmatrix} D_0 \\ D_1 \\ \vdots \\ D_N \end{bmatrix} \quad (10-1-7)$$

It turns out that the simultaneous equations in (10-1-7) may be solved extremely easily. As will be shown later there is little more effort involved than in the use of (10-1-4). The scientist who wishes to solve partial differential equations numerically without becoming a computer scientist is well advised to use the Crank-Nicolson scheme. The extra effort required to figure out how to solve (10-1-7) is well rewarded by the ability to use any  $\Delta x$  and  $\Delta t$  and to forget about stability and the biasing effects of noncentral differences.

Now let us consider heat flow in two spatial dimensions. The heat-flow equation becomes

$$\frac{\partial T}{\partial t} = \frac{\sigma}{C} \left( \frac{\partial^2 T}{\partial x^2} + \frac{\partial^2 T}{\partial y^2} \right) \quad (10-1-8)$$

A simple, effective means to solve this equation is the splitting method. One uses two different equations at alternate time steps. They are

$$\frac{\partial T}{\partial t} = \frac{2\sigma}{C} \frac{\partial^2 T}{\partial x^2} \quad (\text{all } y) \quad (10-1-9a)$$

$$\frac{\partial T}{\partial t} = \frac{2\sigma}{C} \frac{\partial^2 T}{\partial y^2} \quad (\text{all } x) \quad (10-1-9b)$$

Each of these equations (10-1-9a) and (10-1-9b) may be solved by the Crank-Nicolson method.

There are much fancier methods than the splitting method, but their truncation errors (the asymptotic difference between the difference equation and the differential equation) do not go to zero any faster than the truncation error for the splitting method.

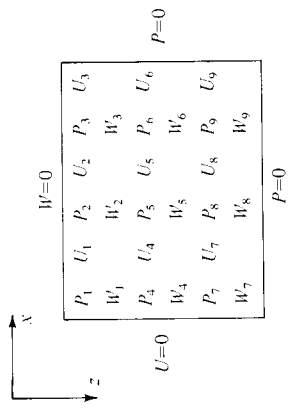


FIGURE 10-1

A grid arrangement for the acoustic equation. This arrangement avoids the necessity of taking  $\partial_x$  or  $\partial_z$  over more than one interval. It also results in (10-1-12) being a scalar equation rather than a  $2 \times 2$  block matrix equation.

Now let us see how to formulate the acoustical problem in a Crank-Nicolson form. Let  $u$  and  $w$  denote velocities in the  $x$  and  $z$  directions. Let  $P$  denote pressure,  $\rho$  denote density, and  $K$  denote incompressibility. Acceleration equal to pressure gradient gives

$$\rho \frac{\partial u}{\partial t} = -\frac{\partial P}{\partial x}$$

$$\rho \frac{\partial w}{\partial t} = -\frac{\partial P}{\partial z}$$

and pressure decreasing with the divergence of velocity gives

$$\frac{\partial P}{\partial t} = -K \left( \frac{\partial u}{\partial x} + \frac{\partial w}{\partial z} \right)$$

Arranging into a matrix and letting  $\partial_x$  denote  $\partial/\partial x$ , etc., we have

$$\frac{\partial}{\partial t} \begin{bmatrix} P \\ U \\ W \end{bmatrix} = \begin{bmatrix} 0 & -K\partial_x & -K\partial_z \\ -\rho^{-1}\partial_x & 0 & 0 \\ -\rho^{-1}\partial_z & 0 & 0 \end{bmatrix} \begin{bmatrix} P \\ U \\ W \end{bmatrix} \quad (10-1-10)$$

The implementation of (10-1-10) by a Crank-Nicolson scheme follows in a direct analogy to the implementation of (10-1-3). The principal difference is that we have vectors and matrices in (10-1-10) but only scalars in (10-1-3). When the splitting method is applied to (10-1-10) we have

$$\frac{\partial}{\partial t} \begin{bmatrix} P \\ U \end{bmatrix} = 2 \begin{bmatrix} 0 & -K\partial_x \\ -\rho^{-1}\partial_x & 0 \end{bmatrix} \begin{bmatrix} P \\ U \end{bmatrix} \quad (10-1-11a)$$

and

$$\frac{\partial}{\partial t} \begin{bmatrix} P \\ W \end{bmatrix} = 2 \begin{bmatrix} 0 & -K\partial_z \\ -\rho^{-1}\partial_z & 0 \end{bmatrix} \begin{bmatrix} P \\ W \end{bmatrix} \quad (10-1-11b)$$

at alternate time steps. When formulating boundary conditions for (10-1-11a) it turns out to be convenient to define  $P$  and  $U$  on alternate squares of a checkerboard. See Fig. 10-1.

A final matter of great practical significance is the fast method of solution to a tri-diagonal set of simultaneous equations like (10-1-6) or (10-1-7). A slightly more general set of equations is

$$A_k T_{k+1} + B_k T_k + C_k T_{k-1} = D_k \quad (10-1-12)$$

For the heat-flow equation the elements of (10-1-12) are scalars. In other physical problems we may have to regard  $A$ ,  $B$ , and  $C$  as  $2 \times 2$  matrices,  $T$  as a  $2 \times 1$  vector for each  $k$  at the  $n+1$  time level, and  $D_k$  as a  $2 \times 1$  vector function of the field variables known at the  $n$  time level. The method proceeds by writing down another equation ( $E_k$ ,  $F_k$  yet unknown) with the same solution  $T_k$  as (10-1-12)

$$T_k = E_k T_{k+1} + F_k \quad (10-1-13)$$

Write (10-1-13) with shifted index

$$T_{k-1} = E_{k-1} T_k + F_{k-1} \quad (10-1-14)$$

Insert into (10-1-12)

$$A_k T_{k+1} + B_k T_k + C_k (E_{k-1} T_k + F_{k-1}) = D_k \quad (10-1-15)$$

Rearrange (10-1-15) to resemble (10-1-13)

$$T_k = -(B_k + C_k E_{k-1})^{-1} A_k T_{k+1} + (B_k + C_k E_{k-1})^{-1} (D_k - C_k F_{k-1}) \quad (10-1-16)$$

Comparing (10-1-16) to (10-1-13) we see that they are the same, so that  $E_k$  and  $F_k$  may be developed by the recursions

$$E_k = -(B_k + C_k E_{k-1})^{-1} A_k \quad (10-1-17a)$$

$$F_k = (B_k + C_k E_{k-1})^{-1} (D_k - C_k F_{k-1}) \quad (10-1-17b)$$

Naturally when doing this on a computer for any case where matrices contain zeros, as in (10-1-11), one should use this fact to simplify things.

Now we consider boundary conditions. Suppose  $T_0$  is prescribed. Then we may satisfy (10-1-13) with  $E_0 = 0$ ,  $F_0 = T_0$ . Then compute all  $E_k$  and  $F_k$ . Then if  $T_N$  is prescribed, we may use (10-1-13) to calculate successively  $T_{N-1}$ ,  $T_{N-2}$ , ...,  $T_0$ . Another useful set of boundary conditions is to prescribe the ratios  $r_1 = T_0/T_1$  and  $r_2 = T_N/T_{N-1}$ . Begin by choosing  $E_0 = r_1$ ,  $F_0 = 0$ . Compute  $E_k$  and  $F_k$ . Then solve the following for  $T_N$ . From (10-1-14)

$$T_{N-1} = E_{N-1} T_N + F_{N-1}$$

$$T_N/r_2 = E_{N-1} T_N + F_{N-1}$$

$$T_N = \left( \frac{1}{r_2} - E_{N-1} \right)^{-1} F_{N-1}$$

Then compute  $T_{N-1}$ ,  $T_{N-2}$ , ..., as before.

As stated earlier, there are many more details associated with numerical solutions to partial differential equations. This chapter has given only the most important tricks for initial-value problems. A program to solve tri-diagonal simultaneous equations is given in Fig. 10-2.

```

SUBROUTINE TRI(A,B,C,N,T,D,E,F)
DIMENSION T(N),D(N),F(N),E(N)
N1=N-1
E(1)=1.0
F(1)=0.
DO 10 I=2,N1
DEN=B+C*E(I-1)
E(I)=-A/DEN
F(I)=(D(I)-C*F(I-1))/DEN
T(N)=F(N1)/(1.0-E(N1))
DO 20 J=1,N1
I=N-J
T(I)=E(I)*T(I+1)+F(I)
RETURN
END

```

FIGURE 10-2  
A program to solve tri-diagonal simultaneous equations.  $A$ ,  $B$ , and  $C$  are assumed independent of  $k$  and zero-slope end conditions are used.

## EXERCISES

- 1 Consider solving (10-1-8) by a Crank-Nicolson scheme in two dimensions on a  $4 \times 4$  grid. This leads to a  $16 \times 16$  set of simultaneous equations for the unknown  $T_{j,k}^n$ . What is the pattern of zeros in the  $16 \times 16$  matrix? The difficulty in actually solving this set gives impetus to the splitting method.
- 2 A difference approximation to the heat-flow partial differential equation is

$$P_j^{n+1} - P_j^{n-1} = \frac{a \Delta t (P_{j+1}^n - 2P_j^n + P_{j-1}^n)}{\Delta x^2} + s_j^n$$

utilizing the trial solution  $P_j^n = Q_n e^{ikj \Delta x}$  reduce the equation to a one-dimensional difference equation. Write the reduced equation in terms of  $Z$  transforms. Does this equation correspond to a nondivergent filter for any real values of  $a$ ? for any imaginary values of  $a$ ? (Use a Fourier expansion for  $s_j$ .)

- 3 Modify the computer program of Fig. 10-2 so that instead of prescribing zero-slope end conditions, (10-1-7) is solved.
- 4 Write a computer program to solve equation (10-1-6) with  $b = .5$  and initial conditions  $T(1) \cdots T(20) = 0.0$  and  $T(21) \cdots T(30) = 1.0$ . Use subroutine TRI.

## 10-2 WAVE EXTRAPOLATION IN OPTICS

In geophysics we generally have measurements along a line on the surface of the earth ( $x$  axis) from which we like to make deductions about earth properties below the surface. The first step is often to extrapolate observations at the earth's surface in a downward direction.

Before looking at numerical methods of extrapolating wave fields in space it will be valuable to review quickly the methods used in optics to extrapolate waves through microscopes and telescopes. An enjoyable, more complete account will be found in Reference 35.

We will take a wave disturbance in two-dimensional cartesian geometry  $p(x, z, t)$  given at  $z_0$  and show how it is extrapolated down the optic axis. Three common situations arise in the projection of a beam of light down an optic axis. First is the projection of a beam through an aperture or a photographic trans-

parency. All that is required for a mathematical description is a transmittance function which ranges from 0 to 1 over the aperture or transparency. Taking the optic axis to be the  $z$  axis and restricting attention to two-dimensional geometry, the projection through an absorber  $T(x)$  located at  $z_0 + dz/2$  is

$$p(t, x, z_0 + dz) = T(x)p(t, x, z_0) \quad (10-2-1)$$

The second common situation is projection through a lens, often approximated as a "thin lens." Here it is necessary to define a differential delay function  $\tau(x)$  which describes the time delay on propagation through the lens of a ray at  $x$  parallel to the  $z$  axis. If the lens is located at  $z_0 + dz/2$ , convolution of the wave field with a delayed impulse is represented as

$$\begin{aligned} p(t, x, z_0 + dz) &= \int p(t - s, x, z_0) \delta[s - \tau(x)] ds \\ &= p[t - \tau(x), x, z_0] \end{aligned} \quad (10-2-2a)$$

This time shifting is simply expressed in the frequency domain where the convolution (10-2-2a) becomes a product. Then

$$P(\omega, x, z_0 + dz) = P(\omega, x, z_0) e^{i\omega\tau(x)} \quad (10-2-2b)$$

The third common situation in optics is the projection of waves across a region of empty space. Surprisingly, this is the most difficult of the three projections. First we recall the wave equation

$$\left( \partial_{xx} + \partial_{zz} - \frac{1}{v^2} \partial_{tt} \right) p(t, x, z) = 0 \quad (10-2-3)$$

Taking the velocity  $v$  to be a constant in time and space, we may use the trial solution

$$p(t, x, z) = P(\omega, k_x, z) e^{-i\omega t + ik_x x}$$

which reduces (10-2-3) to the ordinary differential equation

$$\frac{d^2}{dz^2} P = \left( -\frac{\omega^2}{v^2} + k_x^2 \right) P \quad (10-2-4)$$

This equation has two solutions,  $e^{ik_z z}$  and  $e^{-ik_z z}$ , where

$$k_z = \left( \frac{\omega^2}{v^2} - k_x^2 \right)^{1/2} \quad (10-2-5)$$

One of these solutions is a wave down the  $z$  axis and the other is a wave going up the axis. Initial conditions (and the no-backscattering approximation at lenses and apertures) enable us to reject one of the solutions, leaving us with

$$\begin{aligned} P(\omega, k_x, z) &= P(\omega, k_x, z_0) e^{ik_z(z - z_0)} \\ &= P(\omega, k_x, z_0) e^{i(\omega^2/v^2 - k_x^2)^{1/2}(z - z_0)} \end{aligned} \quad (10-2-6)$$

The right-hand side is a product of two functions of  $k_x$ . It is also the product of two functions of  $\omega$ . This means that with the standard tools of Fourier analysis we

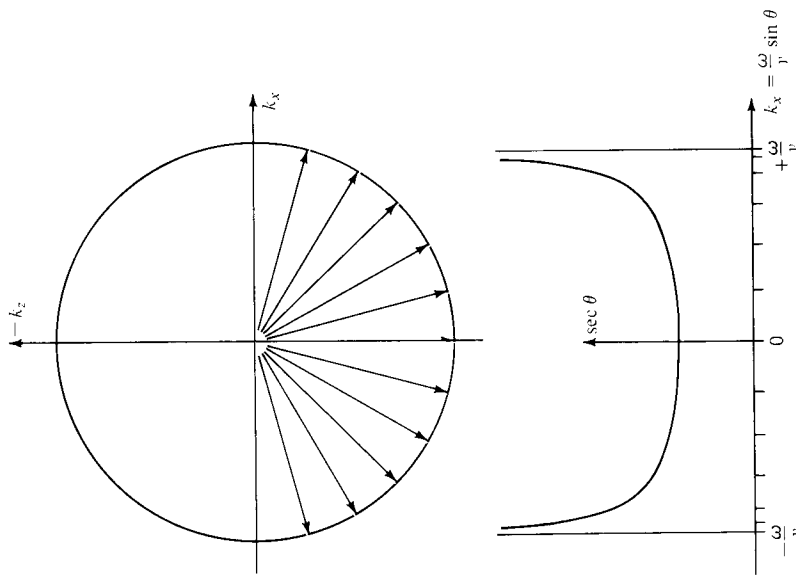


FIGURE 10-3

Power spectrum in  $k_x$  for an isotropic distribution of rays from a point source. Around  $\theta = \pm 90^\circ$  there is a clustering of rays at  $k_x = \pm \omega/v$ . Power as a function of  $k_x$  will be proportional to  $d\theta/(dk_x/d\theta) = d\theta/(d \sin \theta/d\theta) = d\theta/\cos \theta = [1 - (\omega k_x/\omega)^2]^{-1/2} d\theta$ . This result may be compared to the transfer function (10-2-7) which has a constant magnitude for  $-\omega/v < k_x < \omega/v$ .

could recast (10-2-6) to a convolution in either the time domain or the space domain  $x$  or both. Converting the "filter" transfer function

$$\exp i \left( \frac{\omega^2}{v^2} - k_x^2 \right)^{1/2} (z - z_0) \quad (10-2-7)$$

to the space domain will give us an "impulse response" which in this case has the physical meaning of the wave field transmitted through a point aperture. A beam emerging from a point aperture behaves somewhat like a beam from a point source. To recognize the difference, note that the transfer function (10-2-7) has a unit magnitude independent of  $k_x$  but, from Fig. 10-3, the spectral magnitude of a point source is lower near  $k_x = 0$  and peaks up around  $k_x = \pm \omega/v$ . This means that the aperture function does not radiate isotropically like the point source but

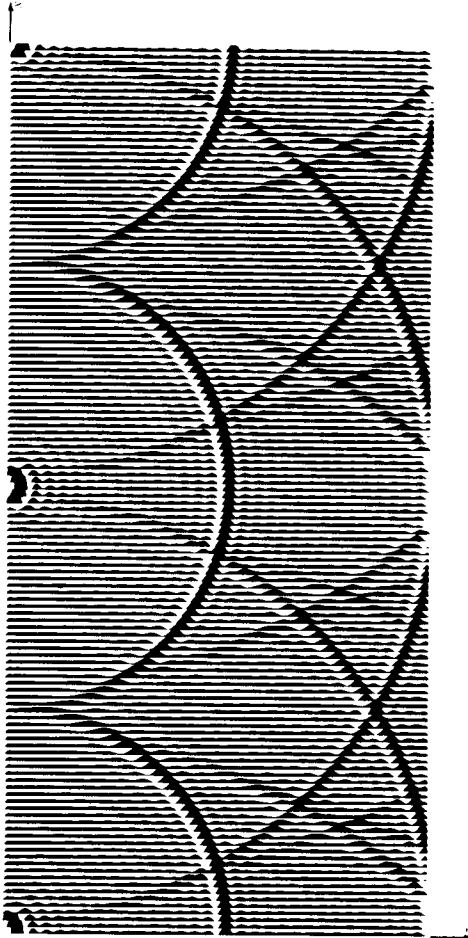


**FIGURE 10-4**  
A snapshot of the wave-equation transfer function. A double Fourier sum of  $\exp[i(\omega^2/v^2 - k_x^2)^{1/2}z]$  was done over  $k_x$  and  $\omega$ . We see a display of the  $(x, z)$  plane at a fixed  $t$ . The result is semi-circular wavefronts with amplitude greatest for waves propagating along the  $z$  axis. Periodicity in  $x$  and  $t$  results from approximating Fourier integrals by sums.

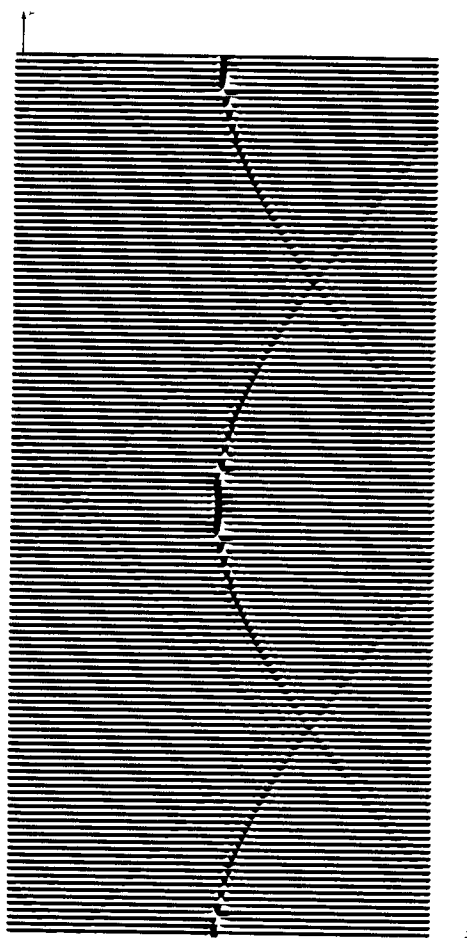


**FIGURE 10-5**  
Seismic profile type displays of the wave-equation transfer function. A double Fourier sum of (10-2-7) was done over  $k_x$  and  $\omega$ . As with a collection of seismograms, we see the  $(x, t)$  plane for a fixed  $z_0$ . The hyperbolic arrival times measure the distance from a point aperture at  $(0, 0)$  to the screen  $(x, z_0)$ . Ray theory easily explains the travel time, but the slow amplitude decay along the hyperbola, an obliquity function, is a diffraction phenomenon not easily computed by analytic means, especially far off axis. The obliquity function should not be confused with the hash which arises from attempted representation of a delta function on a grid.

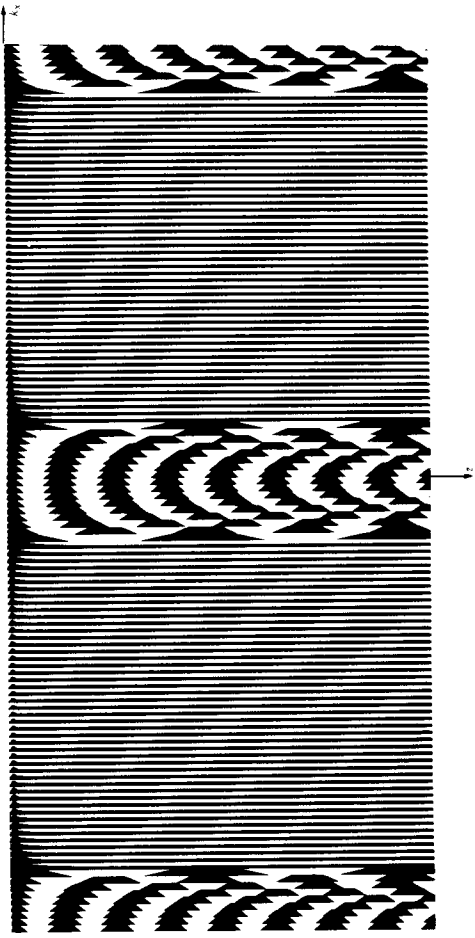


**FIGURE 10-6**  
The real part of the exact transfer function,  $\exp[i\sqrt{(\omega^2/v^2) - k_x^2}z]$ , plotted  $k_x$  vs.  $z$  with  $\omega$  taken as constant. The abrupt change in character of the function occurs at  $\omega^2/v^2 = k_x^2$ , the transition between propagation and evanescence.

contains more energy near  $k_x = 0$ , which is energy directed along the  $z$  axis. There seems to be no easy analytical procedure for the Fourier transformation of (10-2-7) into time and space domains. One of my associates, Philip Schultz, did some numerical Fourier transforms to obtain the display's real parts shown in Figs. 10-4, 10-5, and 10-6. Sample data Fourier transforms induce periodicity in all the transformed coordinates. The periodicity is quite apparent, and there has been no attempt to suppress it in the figures.

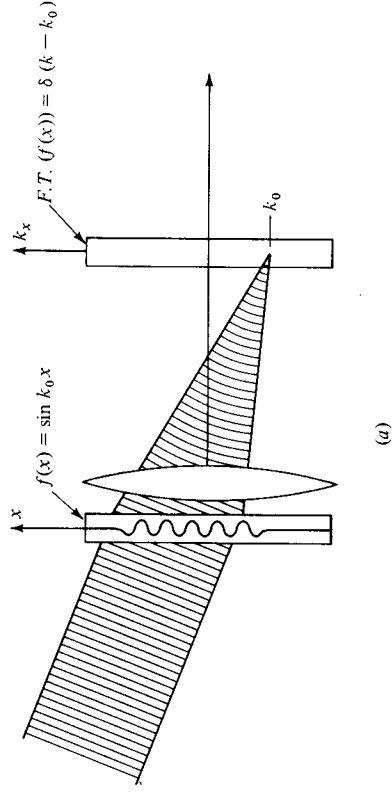
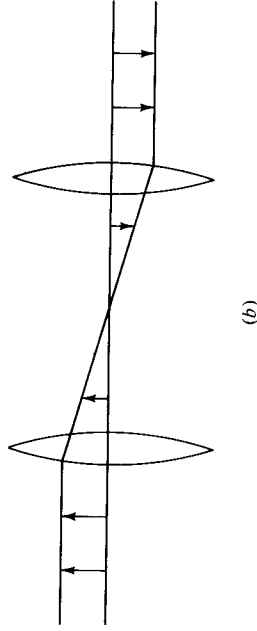


**FIGURE 10-7a**  
Fourier transformation by a lens. A sinusoidal oscillation in the  $x$  domain results from a beam propagating through at some angle. A lens then converts the beam to a point in the  $k_x$  domain. The Fourier transform of a sinusoid is a delta function. The shift of the delta function from the optic axis is in proportion to the rate of oscillation of the sinusoid.



(b)

FIGURE 10-7b  
Two lenses separated by twice their focal length can be used to invert an image. Two Fourier transforms can be used to reverse a function.

It is well known that a lens can be used to take a Fourier transform. Actually a Fourier transform takes place when a beam is allowed to propagate to infinity. The lens just serves to bring infinity back into range. Suppose a monochromatic optical disturbance  $P(x, z, \omega)$  is observed at  $z_0$ . This function of  $x$  may be expanded in a Fourier integral of components of the form  $A(k_x)e^{ik_x x}$ . The important thing is to recognize that any single component represents a plane wave propagating at an angle  $\sin \theta = vk_x/\omega$  from the  $z$  axis. On propagation to a screen the largest values of  $k_x$  project farthest from  $x = 0$ . Figure 10-7a exhibits this idea where a lens is used. That two lenses invert an image is the physical manifestation of the mathematical fact that a Fourier transform is not its own inverse. The inverse transform has an opposite signed exponential. One can readily verify that transforming twice with the same signed exponential just reverses the original waveform. The situation is depicted in Fig. 10-7b.

### 10-3 NUMERICAL EXTRAPOLATION OF MONOCHROMATIC WAVES

The optical method of wave extrapolation is not valid in materials for which the wave velocity  $v = v(x, z)$  is space variable because then the complex exponential function does not turn out to be a valid solution to the wave equation. For this reason we will now seek a numerical procedure for extrapolating wave fields which does not depend on analytic solutions or any particular velocity distribution. The assumption of monochromatic solutions  $e^{-i\omega t}$  reduces the wave equation to the Helmholtz equation

$$P_{xx} + P_{zz} = \frac{-\omega^2}{v(x, z)^2} P \quad (10-3-1)$$

Now let us think about using (10-3-1) to extrapolate  $P(x, z_0)$  in the  $z$  direction. Say we know  $P$  at  $z_0$  for all  $x$ . Then we can find  $P_{zz}$  by rearrangement of (10-3-1)

$$P_{zz} = -\frac{\omega^2}{v^2} P - P_{xx} \quad (10-3-2)$$

Given  $P$  and  $P_z$  for all  $x$  at some particular  $z$  with the help of (10-3-2) we might theoretically expect that we would be able to use a finite differencing scheme to obtain  $P$  and  $P_z$  at  $z + \Delta z$ . Actually, a fundamental difficulty is sneaking up on us. To understand it, let us assume  $v$  is a constant independent of  $x$  and that we have Fourier transformed the  $x$  dependence to  $k_x$  dependence. Then (10-3-2) becomes

$$P_{zz} = \left( -\frac{\omega^2}{v^2} + k_x^2 \right) P \quad (10-3-3)$$

The behavior of (10-3-3) will be dramatically affected by the sign of the factor  $-\omega^2/v^2 + k_x^2$ . If it is positive, we will have growing and decaying exponential solutions. If it is negative, we will have nice, sinusoidal, wavelike solutions. Numerically the growing exponential solutions will present problems. These growing solutions can be kept from getting out of sight if we can start the growing exponential function with zero amplitude. This can be arranged by prescribing a certain ratio between  $P$  and  $P_z$ . Actually, come to think of it, geophysically we usually measure only  $P$  anyway and we do not measure  $P_z$ , so why not figure out theoretically a value of  $P_z$  from  $P$  which avoids the growing solution? Furthermore, in optics the extrapolation of  $P(x, z_1)$  to  $P(x, z_2)$  does not depend on knowledge of the derivative  $P_z(x, z_1)$ . The wave equation is second order in  $z$  and hence has two solutions (upgoing and downgoing). Thus two boundary conditions are required. In the usual boundary-value problems in physics, solutions are required in the intermediate region between  $z_0$  and  $z_N$  and the appropriate boundary conditions are to prescribe  $P$  at  $z_0$  and  $P$  at  $z_N$ . How does the optical method succeed in avoiding the need for either  $P_z$  at  $z_0$  or the need for  $P$  at  $z_N$ ? It succeeds because one of the two solutions was thrown away when  $k_z$  was defined by choosing only one of two possible square roots. Since one solution is left, only one boundary condition is required instead of two. Throwing away one of the solutions amounts to making an assumption about the physical situation which may or may not be valid. The validity of this assumption is always a matter of degree and depends on practical factors. Our present objective is to modify (10-3-2) to build in the common optical assumption that we are only trying to describe waves with a component along the  $+z$  axis, without building in the common optical assumption of a homogeneous medium. Instead of (10-3-2), which is second order in  $z$  and describes waves which go in both plus and minus  $z$  directions, we would like to have an equation which is first order in  $z$  and describes only waves in the  $+z$  direction. Since geophysically we do not observe  $P_z$ , a valuable added bonus would be that such a first-order equation would require only  $P(x)$  as an initial condition, not both  $P$  and  $P_z$ . Geophysically, the "downgoing wave" assumption can often be used when we are describing the wave field emitted from active prospecting equipment, and an "upgoing wave" assumption can often be used to describe subsequent observations. Naturally, in any situation, the validity of these assumptions must be investigated. To describe a plane wave propagating in the  $+z$  direction we may write

$$P(x, z) = Q_0 e^{i(\omega/v)z}$$

Saying that  $Q_0$  is an unknown constant amounts to saying that the wave has unknown amplitude and phase. Next we write

$$P(x, z) = Q(x, z)e^{i(\omega/v)z}$$

Now, " $Q(x, z)$  is approximately a constant function of  $x$  and  $z$ " is a rather fuzzy statement which we will proceed to sharpen up. By restricting  $Q(x, z)$  to slowly variable functions we will be restricting  $P(x, z)$  to wave fields which are near to plane waves propagating in the  $z$  direction. In fact,  $P$  might represent plane waves propagating at a small angle from the  $z$  axis, or it might be a small portion of a spherical wave, or it might be the observed backscattered radiation in a seismic reflection survey, or on 90° rotation of the coordinate system it might describe surface waves.

The ratio  $\omega/v$  occurs often and it is called the spatial frequency of the wave. We define

$$m = \frac{\omega}{v(x, z)} \quad (10-3-4)$$

We also define  $\bar{m}$  as a spatial average of  $m$ .

$$\bar{m} = \frac{\omega}{\bar{v}} \quad (10-3-5)$$

In a material which is homogeneous  $\bar{m}$  will equal  $m$ . With this definition we write the wave disturbance as

$$P(x, z) = Q(x, z)e^{imz} \quad (10-3-6)$$

Now an additional condition to make  $Q(x, z)$  slowly variable with  $z$  is that  $m(x, z)$  be relatively near to  $\bar{m}$ . Let us compute some partial derivatives of (10-3-6)

$$P_x = Q_x e^{imz} \quad (10-3-7a)$$

$$P_{xx} = Q_{xx} e^{imz} \quad (10-3-7b)$$

$$P_z = (Q_z + imQ)e^{imz} \quad (10-3-7c)$$

$$P_{zz} = (Q_{zz} + 2imQ_z - \bar{m}^2 Q)e^{imz} \quad (10-3-7d)$$

Insert (10-3-7b) and (10-3-7d) into (10-3-1) and cancel the exponential, obtaining

$$Q_{xx} + Q_{zz} + 2imQ_z + (m^2 - \bar{m}^2)Q = 0 \quad (10-3-8)$$

Now we make the very important step where we assert that for many applications  $Q$  is slowly variable and  $Q_{zz}$  may be neglected in comparison with  $2imQ_z$ . Dropping the  $Q_{zz}$  term will be called the parabolic approximation or the paraxial approximation. This gives us the desired first-order, hence initial-value, equation in  $z$ .

$$Q_{xx} + 2imQ_z + (m^2 - \bar{m}^2)Q = 0 \quad (10-3-9)$$

In a homogeneous medium, (10-3-9) reduces to

$$Q_{xx} + 2imQ_z = 0 \quad (10-3-10)$$

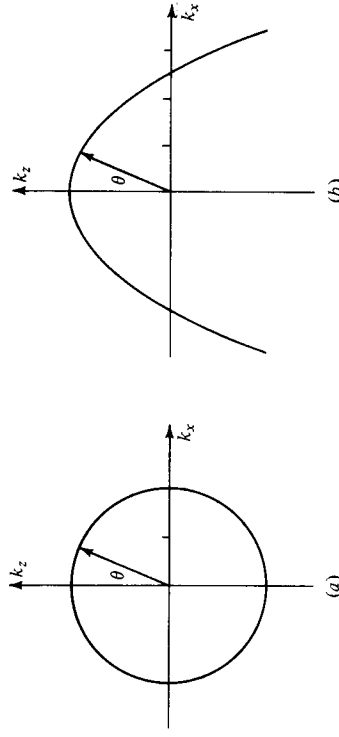


FIGURE 10-8  
Graph of acceptable wave numbers to wave equation (a) and to one-way wave equation (b).

Equation (10-3-10) is really of the same form as the heat-flow equation if  $z$  is associated with time and the heat conductivity is taken to be imaginary. The equation is, in fact, known as the Schroedinger equation. It may be solved numerically by the means described for the heat-flow equation in Sec. 10-1. Ultimately (10-3-10) will be advocated for quite a number of purposes, so before we proceed let us take a look at what we have lost by dropping  $Q_{zz}$ . To facilitate comparison of (10-3-10) to the wave equation, let us convert back from the  $Q$  variable to the  $P$  variable. Rearrange (10-3-6) and form derivatives.

$$Q = P e^{-imz} \quad (10-3-11a)$$

$$Q_{xx} = P_{xx} e^{-imz} \quad (10-3-11b)$$

$$Q_z = (P_z - imP)e^{-imz} \quad (10-3-11c)$$

Insert (10-3-11b) and (10-3-11c) into (10-3-10) and cancel the exponential, getting the equation which we will call the one-way wave equation.

$$P_{xx} + 2im(P_z - imP) = 0$$

$$P_{xx} + 2imP_z + 2\bar{m}^2 P = 0 \quad (10-3-12)$$

One technique which may be used to solve any partial differential equation in cartesian coordinates with constant coefficients is to insert the complex exponential  $e^{i(k_x x + k_z z)}$ . If  $k_x$  and  $k_z$  turn out to be real, then this trial solution may be interpreted as a plane wave propagating in the  $k = (k_x, k_z)$  direction. Inserting this exponential into both the wave equation (10-3-1) and the one-way wave equation (10-3-12) and canceling the exponential, we get two algebraic equations called dispersion relations. They are

$$-k_x^2 - k_z^2 + m^2 = 0 \quad (10-3-13)$$

$$-k_x^2 - 2\bar{m}k_z + 2\bar{m}^2 = 0 \quad (10-3-14)$$

These two equations are graphed in Fig. 10-8, a and b.

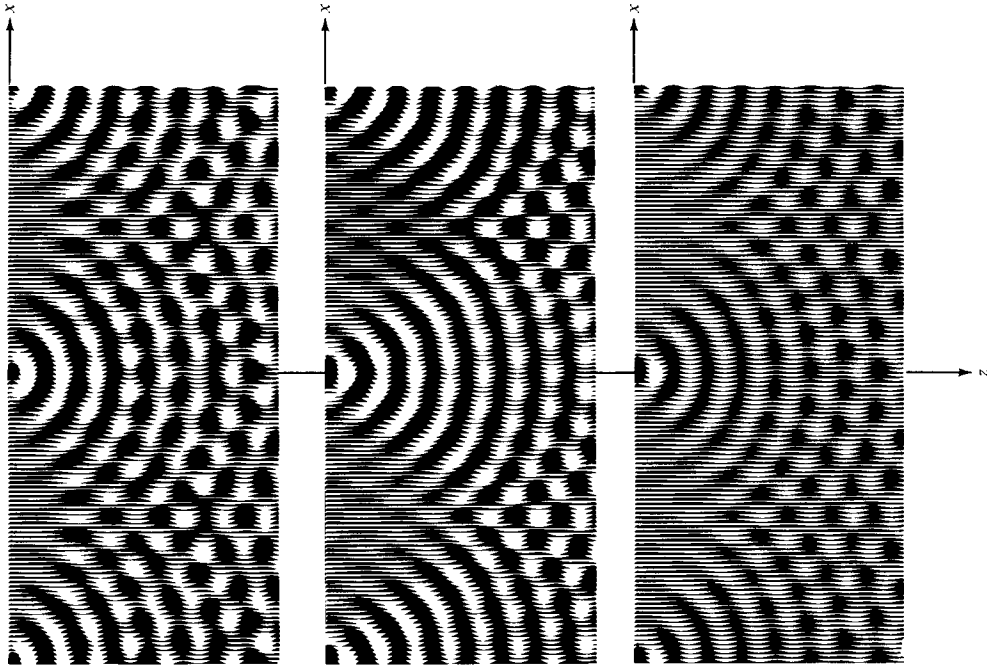


**FIGURE 10-9**  
Snapshots of the monochromatic wave-equation transfer function. A Fourier sum over  $k_x$ , done over the exact wave-equation transfer function  $\exp[i(1 - k_x^2 v^2 / \omega^2)^{1/2} \omega z / v]$ , is displayed (top) in the  $(x, z)$  plane for a fixed frequency  $\omega_0$ . Middle is the same for the 15° approximate transfer function  $\exp[i(1 - k_x^2 v^2 / 2\omega^2) \omega z / v]$ . Bottom is the same for the 45° approximation

$$\exp \left[ i \frac{\omega}{v} \frac{4\omega^2 - 3k_x^2 v^2}{4\omega^2 - k_x^2 v^2} z \right] \text{ of Exercise 2.}$$

The physical picture is of waves passing through small apertures which are periodically spaced along the  $x$  axis.

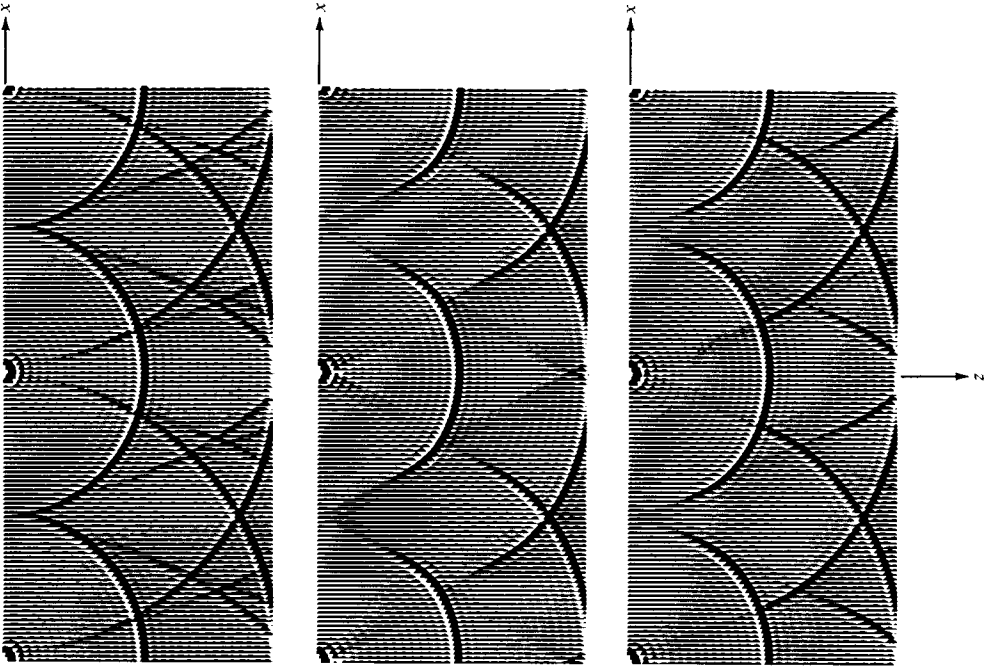


**FIGURE 10-10**  
Snapshots of the time-dependent wave-equation transfer function and approximations. A double Fourier sum over  $k_x$  and  $\omega$  of the functions of Fig. 10-12 shows the  $(x, z)$  plane at a fixed time.

The graph for the wave equation is a circle and illustrates what we already know, namely that the magnitude of the wave number in an arbitrary direction, that is,  $(k_x^2 + k_z^2)^{1/2}$  is equal to the constant  $\omega/v$ . Such is not the case, however, for the one-way wave equation. Here we have only the approximation  $k_x^2 + k_z^2 \approx \omega^2/v^2$  for small angles  $\theta$ . Figure 10-8a also illustrates geometrically that (10-3-14) is an initial-value problem in  $z$  because Fig. 10-8a gives two values for  $k_z$  corresponding to any  $k_x$ , but Fig. 10-8b gives only one value for  $k_z$ . Figures 10-9,



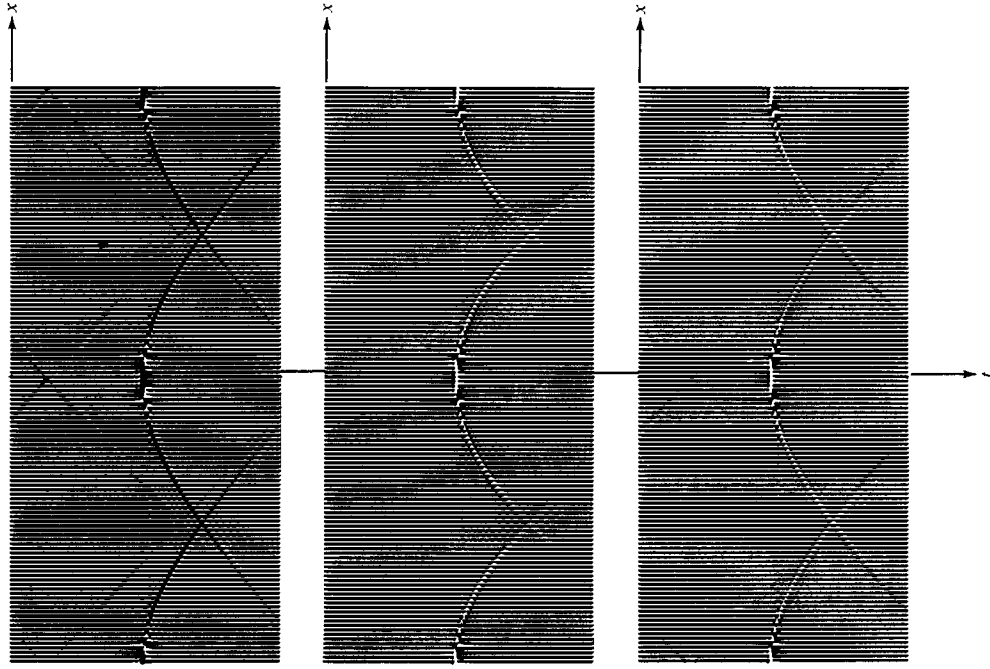


FIGURE 10-11  
Seismic profile-type displays of the wave-equation transfer function and two approximations to it. Exact, 15° approximate, and 45° approximate forms of the wave-equation transfer function were Fourier summed over  $k_x$  and  $\omega$ . As with a seismic profile, we see a display of the  $(x, t)$  plane for a fixed  $z$ . The exact solution (top) is a delta function along a hyperbola. The 15° approximation (middle) is a parabola. The approximations die out more rapidly with angle than the exact solution.

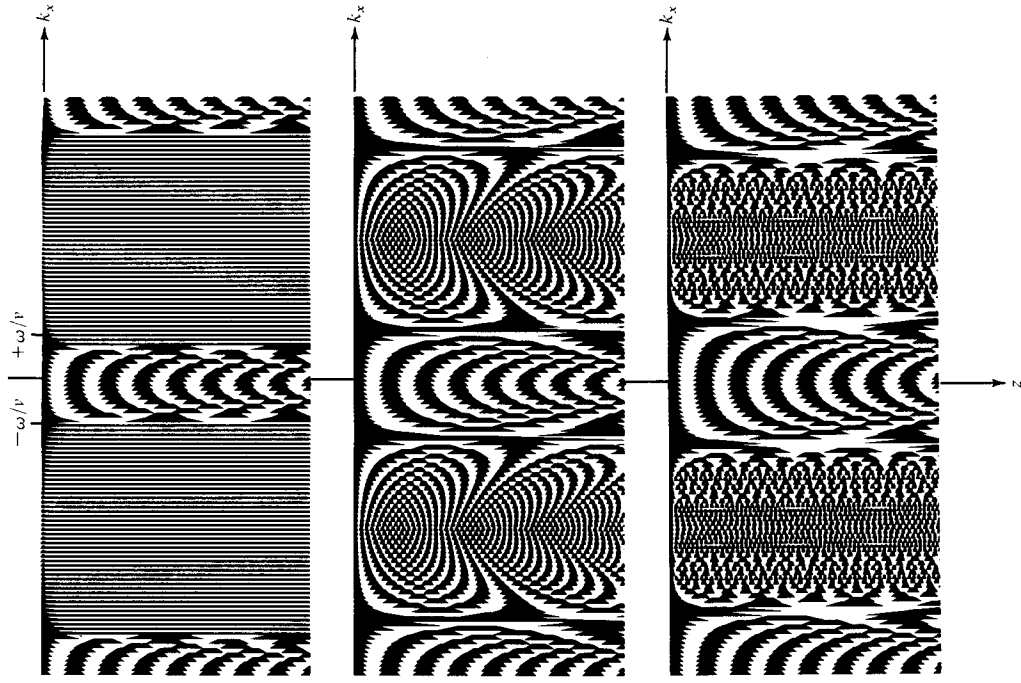


FIGURE 10-12  
Monochromatic wave-equation transfer functions displayed in the plane of  $(k_x, z)$ . The real part only is shown. Top is the exact transfer function. Note the abrupt change to evanescence at  $|k_x v / \omega| = |\sin 90^\circ| = 1$ . The exponential decay for  $k_x > \omega / v$  is perceptible near  $z = 0$ . The 15° approximation (middle) and the 45° approximation (bottom) are all-pass filters and have replaced the evanescent region by an interesting design. In order to eliminate a massive amount of short horizontal wavelength fuzz in the spatial domain on the previous two figures, this evanescent zone was removed with a step function. The implication in a data processing application is that occasionally the approximate transfer functions may well be augmented by a fan-filter. (See Ref. [36].)

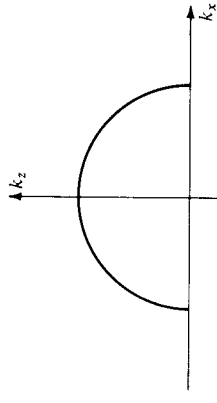


FIGURE 10-13

The dispersion relation for an ideal one-way wave equation is a semicircle.

10-10, 10-11, and 10-12 show the wave equation transformation function  $e^{ik_z z}$  and approximations  $e^{ik_z z}$  and Fourier transformations thereof.

What we really want is a one-way wave equation which has the semicircle of Fig. 10-13 for its dispersion relation. The equation for the perfect semicircle is given by

$$k_z = \sqrt{m^2 - k_x^2} \quad (10-3-15)$$

This of course is the basic relation used for extrapolation in optics. By the binomial expansion, (10-3-15) may be written

$$k_z = m \left( 1 - \frac{k_x^2}{2m^2} - \frac{k_x^4}{8m^4} + \dots \right) \quad (10-3-16)$$

This expression converges for all  $0 < k_x < m$ .

Now for the sudden flash of insight which enables us to write the partial differential equation with this semicircle as its dispersion relation, from (10-3-16) we are inspired to write

$$\partial_z P = im \left( 1 + \frac{\partial_{xx}}{2m^2} - \frac{\partial_{xxxx}}{8m^4} + \dots \right) P \quad (10-3-17)$$

Clearly, insertion of the plane wave  $\exp(ik_x x + ik_z z)$  into (10-3-17) immediately gives the desired semicircular dispersion relation (10-3-16). Thus, the greater the angular accuracy desired the more terms of (10-3-17) are required in the calculation. As a shorthand we may choose to write (10-3-17) as

$$\partial_z P = i(m^2 + \partial_{xx})^{1/2} P \quad (10-3-18)$$

It will be of no help to us, but it turns out that (10-3-18) is the relativistic Schrödinger equation.

It is easy to obtain the wave equation from (10-3-18). Just differentiate with respect to  $z$

$$\partial_{zz} P = i \partial_z (m^2 + \partial_{xx})^{1/2} P$$

Taking  $m$  independent of  $z$ , we may interchange the order of differentiation

$$\partial_{zz} P = i(m^2 + \partial_{xx})^{1/2} \partial_z P$$

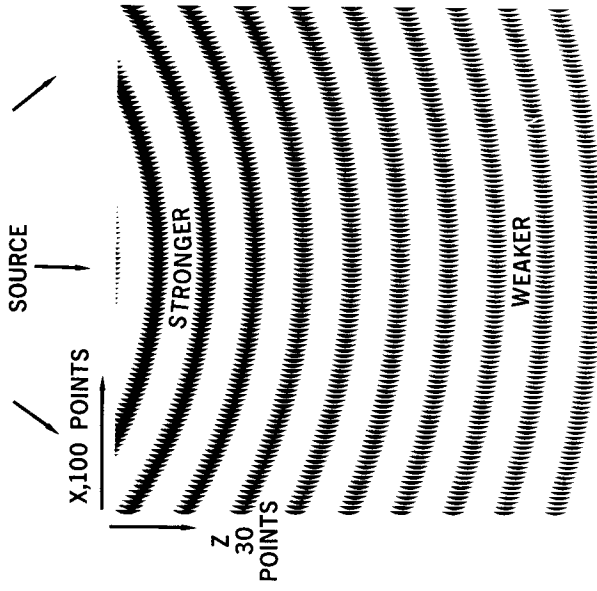


FIGURE 10-14

An expanding monochromatic cylindrical wave. The wavefronts are concentric circles of decreasing amplitude. The computation begins with an analytic solution at the top of the figure in a 100-point linear grid. Using difference equations, we stepped the grid downward, thirty steps making up the whole figure. About six complex multiplications are required per point; this amounts to about five seconds of time on our computer. The display is the  $(x, z)$  plane, although a multichannel seismogram plotter has been used. (From Ref. [3], p. 408.)

inserting (10-3-18)

$$\begin{aligned} \partial_{zz} P &= -(m^2 + \partial_{xx})^{1/2} (m^2 + \partial_{xx})^{1/2} P \\ &= -(m^2 + \partial_{xx}) P \end{aligned}$$

which is the wave equation.

Figures 10-14, 10-15, and 10-16 show finite-difference solutions to the parabolic approximated wave equation in homogeneous media.

Next, let us turn to the question of using the parabolic approximation in the presence of space variations in material velocity. The exercises go into considerable detail on this matter, but we can easily make some improvements over (10-3-9). The main idea is to approximate a circle by a parabola; the actual radius of the circle does not have anything to do with the approximation. This leads to the suggestion that (10-3-12) or (10-3-14) could be used with  $\bar{m}$  replaced by  $m$ , as in (10-3-17); hence (10-3-12) would be

$$P_{xx} + 2im(x, z)P_z + 2m^2(x, z)P = 0 \quad (10-3-19)$$

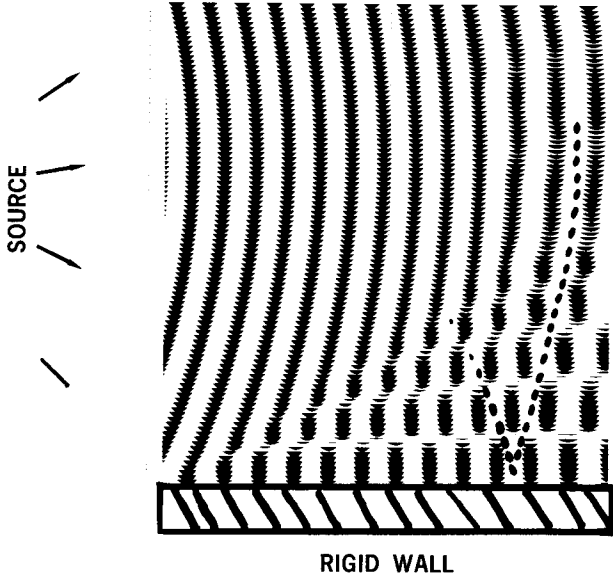


FIGURE 10-15

Like Fig. 10-14, but the left-hand boundary is a rigid wall. Waves may be seen reflecting back into the medium from the boundary. The reflected wavefront is indicated by the shorter of the two dashed lines. (From Ref. [3], p. 409.)

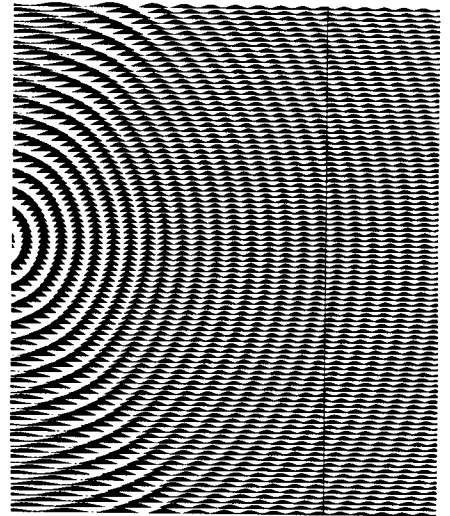


FIGURE 10-16  
Expanding cylindrical wave. A theoretical solution was put in at the top boundary and extrapolated downward with the equation of Exercise 2. The wavefronts are not quite circular as they would be were it feasible to use (10-3-18). Notice also that the theoretical  $r^{-1/2}$  amplitude decay is not exhibited for waves about  $60^\circ$  off the vertical. Such waves attenuate less rapidly because at  $60^\circ$  the phase curve is flatter than a circle. (From Ref. [5], p. 476.)

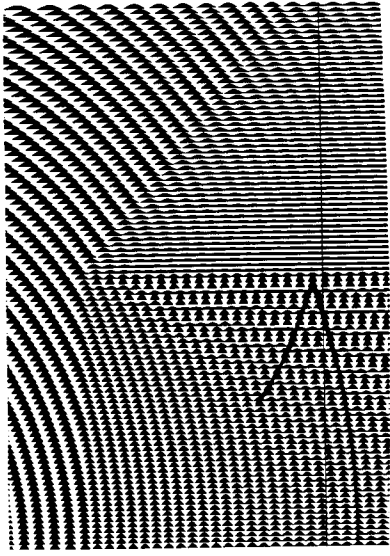


FIGURE 10-17  
Waves impinging on a buried block of low-velocity material. Waves enter at the top of the block and are completely internally reflected from the side of the block. This leaves a shadow on the outside of the block. (From Ref. [5], p. 474.)

With (10-3-19) we no longer need to assume that  $m \approx \bar{m}$  so we can now deal with a wide range of velocities. Actually, as the exercises will show, the validity of (10-3-19) depends also on the approximation that the logarithmic space gradients of material velocity are small compared with the logarithmic gradients of the waves. In other words, the waves change faster than the material does.

Figures 10-17, 10-18, and 10-19 illustrate the propagation of waves in inhomogeneous materials.

The approximation is evidently best at high frequencies (short wavelengths). This approximation is well known in wave theory. Although it is sometimes called a ray approximation, the reader should not fear that the theory has degenerated to geometrical optics. Actually all the phenomena of physical optics (for example: interference, diffraction, and finite size focus) are still present. In fact we need not go to the physical optics limit at all. Some of the exercises are examples that include the velocity gradients found in lower frequency terms. Whether many or none of these terms is important in practice is a question which is particular to each application.

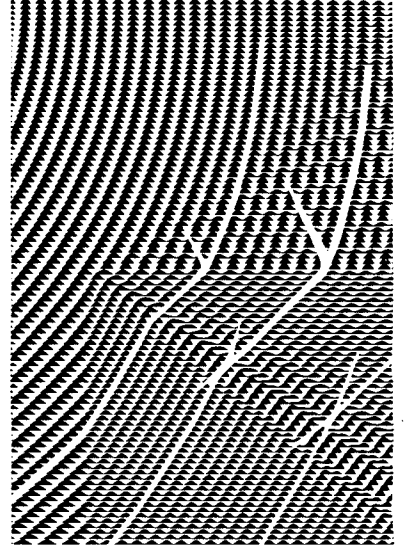


FIGURE 10-18  
A low-velocity block is illuminated from the side. There is partial reflection from the side of the block and interference between waves entering the block through different faces. (From Ref. [5], p. 474.)

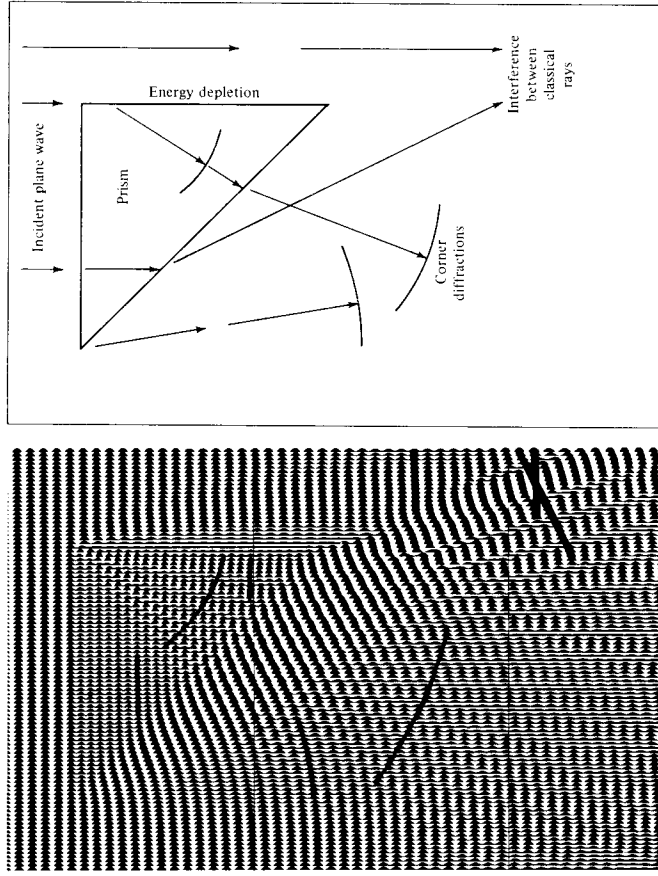


FIGURE 10-19

Plane waves propagating through a right  $45^\circ$  prism. Waves are incident from the top of the page. Shortened wavelength is shown inside the prism. When the waves emerge from the prism they are bent toward the right-hand side of the page. As they emerge, their amplitude increases because they are compressed into a narrower beam. At the bottom right they interfere with waves which have passed along the side of the prism, causing amplitude modulation. Curved wavefronts are the result of diffraction from corners of the prism. Especially interesting is the diffraction from the upper right-hand corner. This is best seen by viewing the figure edge-on from the right-hand edge of the page. The energy for this diffraction is removed from the wave along the right-hand vertical edge of the prism. This calculation requires ten seconds of computer time on the Stanford IBM 360-67. (From Ref. [5], p. 475.)

## EXERCISES

- 1 The variable  $Q$  has the practical advantage over  $P$  because, being more slowly variable with the  $z$  coordinate, it may be sampled less densely, thereby conserving computational effort. Convert (10-3-19) to an equation in  $Q$  by means of (10-3-11). Compare the result to (10-3-9). Of the two equations, yours and (10-3-9), which do you believe to be more accurate? Why?
- 2 An excellent square root approximation is given by the rational expression

$$(1+x)^{1/2} \approx \frac{1+3x/4}{1+x/4}$$

What "one-way wave equation" is suggested by this approximation? Make a graph of the dispersion relation. For selected angles of propagation how does accuracy compare to that of (10-3-14)?

- 3 The algebraic equation  $a + bx + cx^2 = 0$  has two roots. If  $b$  is sufficiently large, we may approximate the smallest root with the linear relation  $a + bx = 0$ . An improved approximation which is still linear in  $x$  may be found by substituting  $x = -a/b$  back into the quadratic

$$a + bx + c \left( \frac{-a}{b} + x \right)^2 = 0$$

$$ab + (b^2 - ac)x = 0$$

- Define  $k_x^2 = m - k_z$  and substitute  $k_z = m - k_x^2$  into  $k_x^2 + k_z^2 = m^2$ . Find the smallest root for  $k_x^2$ . Show that this gives the same partial differential equation as Exercise 2.
- 4 Let the velocity  $v = v(x, z)$  be a function of  $x$  and define  $m = \omega/v(x)$ . Define the operator

$$\text{Op} = m + \frac{1}{2m} \partial_{xx} - \frac{m_x}{2m^2} \partial_x$$

Note that

$$\partial_z P = i \text{Op} P$$

$$\partial_{zz} P = i \partial_z \text{Op} P = i \text{Op} \partial_z P = -\text{Op}^2 P$$

$$(\partial_{zz} + \text{Op}^2)P = 0 = \text{wave equation} + \text{error}$$

Examine each error term and decide whether it is important (1) at high frequencies (collect terms proportional to  $n$ th power of wavelength) and (2) at small or large angles from the  $z$  axis.

- 5 Review the section on Sylvester's matrix theorem. How is the square root of a matrix analogous to the square root of an operator?
- 6 Deduce the "outgoing wave equation" in cylindrical coordinates.
- 7 Deduce the "outgoing wave equation" in spherical coordinates.
- 8 Exercise 3 gave a good wide-angle approximation but Exercise 4 works for  $m = m(x)$ . To utilize the method of Exercise 3 for  $m = m(x)$  it is necessary to note that although  $bx - xb = 0$ , it is not true that  $(m \partial_x - \partial_x m)P = 0$  unless  $m \neq m(x)$ . Salvage the method of Exercise 3 by avoiding the use of commutivity as much as possible.
- 9 Consider surface waves propagating on the surface of an imperfect sphere. Deduce an equation, first-order in  $\phi$ , the longitude coordinate, second-order in  $\theta$ , the latitude coordinate, for waves beamed roughly along the equator. Assume all quantities are independent of the radial coordinate axis.
- 10 Modify the program of Sec. 10-1 in Exercise 4 to compute the solution to (10-3-10). You will need to review the compiler conventions of complex arithmetic. Also, after computing  $Q(x, z)$  multiply it by  $e^{imz}$  to give  $P(x, z)$ . Print only the real part of  $P(x, z)$ . A physical interpretation of this result is light behind an edge of an opaque screen. Waves diffracted into the shadow zone should have semicircular wavefronts if you have arranged your display to preserve  $\Delta z = \Delta x$  on the output.
- 11 Let  $Z = e^{ik_x z}$  denote a discretization of the  $x$  coordinate. Define  $A(Z) = \sum a_n Z^n$  by finding  $a_n$  such that

$$a_0 + \sum_{n=1}^{\infty} a_n \left( Z^n + \frac{1}{Z^n} \right) = |k_x| \quad \text{for } |k_x| \Delta x \leq \pi$$

Show that either solution to

$$\frac{\partial P(Z)}{\partial Z} = \pm A(Z)P(Z)$$

is a solution to Laplace's differential equation  $P_{xx} + P_{zz} = 0$ . These solutions may be used for upward and downward continuation.

### 10-4 EXTRAPOLATION OF TIME-DEPENDENT WAVEFORMS IN SPACE

In Sec. 10-3 we learned how to extrapolate monochromatic waves in space. To extrapolate a time-dependent waveform in space, one could first Fourier transform it into monochromatic waves, then extrapolate them as in the previous section, and finally Fourier transform back into the time domain. Thus, although this section solves, in principle, the same problem as the last section, a direct time-domain method will often be preferable for practical reasons. Although a time-domain study is necessarily more complicated than one in the frequency domain (all time points must be considered together, but each frequency is isolated from the others) there is a great deal more understanding to be gained in the time domain, especially as regards causality. We will discover that wave-extrapolation procedures are like filters (in fact, they are a special kind of multidimensional all-pass filter) and that the feedback parts of these filters must be minimum-phase. There are two independent time-domain derivations.

The first derivation begins by transforming the scalar wave equation

$$0 = P_{xx} + P_{zz} - v^{-2}P_{tt} \quad (10-4-1)$$

into a coordinate frame which translates along the  $z$  axis at the speed  $\bar{v}$  which we will generally take to equal or exceed  $v$ . It does not matter which way energy is propagating in the fixed frame; when it is seen in the moving frame it will remain stationary or fall backward. The coordinate transformation

$$x' = x \quad (10-4-2a)$$

$$z' = \bar{v}t - z \quad (10-4-2b)$$

$$t' = t \quad (10-4-2c)$$

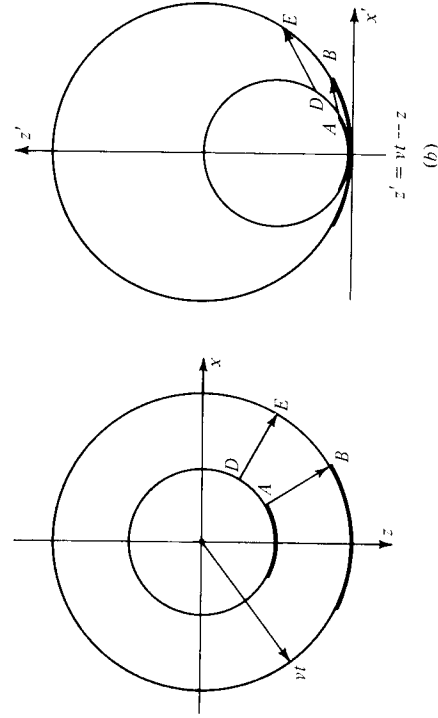


FIGURE 10-20 Expanding spherical wave in (a) fixed coordinates (left) and in (b) coordinates which translate in the  $z$  direction with the velocity of the wave (right).

is depicted in Fig. 10-20 for  $\bar{v} = v$ . In the primed frame all waves have a velocity component in the plus  $z'$  direction. Knowledge of  $P$  for present and past time at all  $x'$  for fixed  $z'$  should be sufficient to determine  $P$  for present and past values of time at  $(x', z' + \Delta z')$  because before anything happens at  $z' + \Delta z'$  something has to happen at  $z'$ . Thus, because of the restriction  $\bar{v} \geq v$  we anticipate that the linear operators which we will develop to extrapolate  $P$  in the plus  $z'$  direction should be causal. Let  $P'$  denote the disturbance in the moving frame. We have

$$P(x, z, t) = P'(x', z', t') \quad (10-4-3)$$

It will be convenient to use subscripts to denote partial derivatives. Obviously,

$$P_x = P'_{x'} \quad \text{and} \quad (10-4-4)$$

$$P_{xx} = P'_{x'x'}$$

Also

$$P_z = P'_{x'}x'_z + P'_{z'}z'_z + P'_{t'}t'_z = -P'_{z'}$$

so

$$P_{zz} = P'_{z'z'} \quad (10-4-5)$$

and

$$P_t = P'_{x'}x'_t + P'_{z'}z'_t + P'_{t'}t'_t = \bar{v}P'_{z'} + P'_{t'}$$

so

$$\begin{aligned} P_{tt} &= \bar{v}(\bar{v}P'_{z't'} + P'_{t'z'}) + \bar{v}P'_{z't'} + P'_{t't'} \\ &= \bar{v}^2P'_{z't'} + 2\bar{v}P'_{z't'} + P'_{t't'} \end{aligned} \quad (10-4-6)$$

Now we may insert (10-4-4), (10-4-5), and (10-4-6) into (10-4-1) and we obtain

$$P'_{x'x'} + \left[1 - \left(\frac{\bar{v}}{v}\right)^2\right]P'_{z'z'} - 2\frac{\bar{v}}{v^2}P'_{z't'} - \frac{1}{\bar{v}^2}P'_{t't'} = 0 \quad (10-4-7)$$

We will take up the constant velocity case  $v(x, z) = \bar{v}$ . The case  $v \neq \bar{v}$  is left for the exercises. Our main interest in (10-4-7) is with those waves which propagate with approximately the velocity of the new coordinate frame. In the moving frame such waves are doppler shifted close to zero frequency. This suggests omitting the  $P'_{t't'}$  term from (10-4-7). Thus (10-4-7) becomes

$$P'_{z'z'} = \frac{v}{2}P'_{x'x'} \quad (10-4-8)$$

If we Fourier transform out the time coordinate equation (10-4-8) becomes  $-i\omega P'_{z'} = (v/2)P'_{x'x'}$  which is identical to the monochromatic equation

$$Q_{xx} + 2imQ_z = 0$$

derived in the preceding chapter. Thus, dropping the  $P'_{t't'}$  term is the familiar approximation of a circle by a parabola.

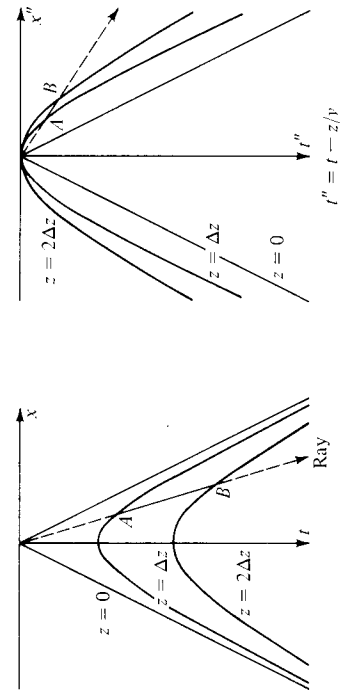


FIGURE 10-21  
 A point-source at  $x = 0, z = 0, t = 0$ . Hyperbolas at left indicate arrival times  $t$  at  $z = 0, \Delta z, 2\Delta z$ . When time is a function of position as given by  $t'' = t - z/v$  the arrival times  $t''$  are as indicated on the right. Energy moves in the direction of  $+t'$ , since on a wavefront  $z = vt \cos \theta$  and we have  $t'' = t - z/v = t(1 - \cos \theta)$ .

In solving (10-4-8) in a computer we can take either of two points of view. The first point of view is that  $P'$  is prescribed initially on a grid over  $x'$  and  $z'$  and then the equation is used for extrapolation in  $t'$ . The second point of view is that  $P'$  is prescribed initially on a grid over  $x'$  and  $t'$  and then (10-4-8) is used for extrapolation in  $z'$ .

Before developing a numerical method for the solution to (10-4-8) we will derive it by means of an entirely different coordinate transformation. Let us take the new coordinate frame fixed in space relative to the old one. However, let a different clock be used at each point in space in the new frame. The clocks all run at the same speed, but they are initialized in such a way that a plane wave traveling in the  $+z$  direction will have the same arrival time measured at all clocks. (This is somewhat like a westward moving jet plane.) The transformation equations are

$$\begin{aligned} x'' &= x & (10-4-9a) \\ z'' &= z & (10-4-9b) \\ t'' &= t - \frac{z}{v} & (10-4-9c) \end{aligned}$$

A disturbance initiated at  $(x, z, t) = 0$  is depicted in Fig. 10-21. Referencing time with respect to the time of the earliest possible ray is a great computational convenience. It means the wave onset does not move off the finite, perhaps short, computational grid on which a wave packet has been defined. Define the disturbance in the new frame by  $P''$  where

$$\begin{aligned} P(x, z, t) &= P''(x'', z'', t'') & (10-4-10) \\ P_{xx} &= P''_{x''x''} & (10-4-11) \\ P_{zz} &= P''_{z''z''} - 2v^{-1}P''_{t''z''} + v^{-2}P''_{t''t''} & (10-4-12) \\ P_{tt} &= P''_{t''t''} & (10-4-13) \end{aligned}$$

Proceeding as before, we obtain

Inserting these into the wave equation (10-4-1) we obtain

$$P''_{t''z''} = \frac{v}{2} (P''_{x''x''} + P''_{z''z''}) \quad (10-4-14)$$

The last term of (10-4-14) is higher-order small for waves traveling at small angles from the  $z$  axis; this recalls that the solution to the wave equation for waves in the  $+z$  direction is an arbitrary function  $f(t - z/v) = f''(t'')$ . Thus  $\partial f''/\partial z''$  vanishes for a wave along the  $z''$  axis. Neglecting  $P''_{z''z''}$  we find that (10-4-14) reduces to

$$P''_{t''z''} = \frac{v}{2} P''_{x''x''} \quad (10-4-15)$$

which is the same equation as (10-4-8). Use of  $e^{-i\omega t}$  time dependence in either (10-4-8) or (10-4-15) yields the equation (10-3-10) which was developed for extrapolation of monochromatic waves. Another point of view is that we could have obtained the time-dependent equations of this chapter by merely replacing  $-i\omega$  in the monochromatic equations with  $\partial_t$ .

Now we develop a differencing scheme for the solution to (10-4-8) or (10-4-15). Drop primes. Let  $j \Delta t$  refer to time. Let  $n \Delta z$  refer to the coordinate  $z$ . Let  $\delta$  denote a difference operator. Let  $\mathbf{P}^j$  be a vector at each value of  $n$  and  $j$ . Running down the vector will be values of pressure along the  $x$  axis. By using matrix algebra we avoid writing a subscript for the  $x$  dependence. Let  $\mathbf{T}$  denote a tridiagonal matrix with the negative of the second difference operator  $-(1, -2, 1)$  on the diagonal. With all these definitions (10-4-8) or (10-4-15) becomes

$$\delta_z \delta_t \mathbf{P}^j = -\frac{v \Delta z \Delta t}{8 \Delta x^2} \mathbf{T} \mathbf{P}^j \quad (10-4-16)$$

Let us define  $a = v \Delta z \Delta t / 8 \Delta x^2$ . Now we must decide more precisely what first-difference approximations to use in (10-4-16). We will use the Crank-Nicolson scheme which is equivalent to the bilinear transform. First do centered time differencing

$$\delta_z (\mathbf{P}^{j+1} - \mathbf{P}^j) = -a \mathbf{T} (\mathbf{P}^{j+1} + \mathbf{P}^j)$$

and then do centered space differencing

$$(\mathbf{P}^{j+1} - \mathbf{P}^{j+1}) - (\mathbf{P}^j - \mathbf{P}^j) = -a \mathbf{T} (\mathbf{P}^{j+1} + \mathbf{P}^{j+1} + \mathbf{P}^j + \mathbf{P}^j) \quad (10-4-17)$$

From the point of view of computation we assume the unknown is  $\mathbf{P}^{j+1}$  and that all else is known. Bringing the unknown to the left and the known to the right, we have

$$(\mathbf{I} + a \mathbf{T}) \mathbf{P}^{j+1} = \mathbf{P}^{j+1} + \mathbf{P}^j - a \mathbf{T} (\mathbf{P}^{j+1} + \mathbf{P}^j) \quad (10-4-18)$$

For each  $n$  and  $j$ , the right side collapses to a known vector. The left side is the tridiagonal matrix  $(\mathbf{I} + a \mathbf{T})$  multiplying the unknown vector  $\mathbf{P}^{j+1}$ . The solution of these equations is extremely simple and may be done as was the heat-flow equation in Sec. 10-1. Boundary conditions in  $x$  are contained on the ends of  $\mathbf{T}$ . For  $z$  and  $t$  boundary conditions it is sufficient to give, at all  $x$ ,  $\mathbf{P}^0_n$  for all  $n$  and  $\mathbf{P}^0_j$  for all  $j$ . Other boundary arrangements are possible.

A very important question is the one of stability. We will now establish that the recursion (10-4-18) is stable for any positive value of  $a$ . If eigenvalues and eigenvectors of  $\mathbf{T}$  were known and if all the  $\mathbf{P}_j^n$  were expanded in terms of the eigenvectors of  $\mathbf{T}$ , then (10-4-18) would decouple into many separate equations, one for each of the eigenvalues of  $\mathbf{T}$ . The eigenvectors of  $\mathbf{T}$  have components which are sinusoidal functions of  $x$ . If there are boundaries in  $x$ , then a discrete set of frequencies is allowed, otherwise there is a continuum. To see this observe that for the unbounded case  $\mathbf{TP}$  is  $(-1, 2, -1)$  convolved with  $e^{ik_x m \Delta x}$  giving

$$(-e^{ik_x \Delta x} + 2 - e^{-ik_x \Delta x})e^{ik_x m \Delta x}$$

Thus the eigenvalue is  $2 - 2 \cos k_x \Delta x = (2 \sin k_x \Delta x / 2)^2$ . Since any eigenvalue must be between 0 and 4 it is sufficient to study (10-4-18) where the vector  $\mathbf{P}_j^n$  has become a scalar  $P_j^n$  function of  $k_x$ ,  $\mathbf{I}$  is replaced by 1, and  $\mathbf{T}$  is replaced by  $T$ , an arbitrary number between 0 and 4. It can be shown that for energy-conserving boundary conditions the eigenvalues are also between 0 and 4. Now, suppose  $P_j^n$  is known for all  $j$  at some particular value of  $n$  and we will investigate the stability of finding  $P_j^{n+1}$  for all  $j$ . Now, in (10-4-17) bring unknowns to the left.

$$(1 + aT)P_{j+1}^{n+1} - (1 - aT)P_j^{n+1} = (1 - aT)P_{j+1}^n - (1 + aT)P_j^n \quad (10-4-19)$$

The important thing for stability in (10-4-19) is that if we are successively increasing  $j$ , then the magnitude of the coefficient of  $P_{j+1}^{n+1}$  must exceed that of the coefficient of  $P_j^{n+1}$ . If we are decreasing  $j$ , the reverse should be true. The stability may be studied by the  $Z$ -transform methods discussed in earlier chapters. By the  $Z$  transform of (10-4-19) we mean that the coefficient of  $Z^j$  of

$$[(1 + aT) - Z(1 - aT)]P(Z)^{n+1} = [(1 - aT) - Z(1 + aT)]P(Z)^n \quad (10-4-20)$$

gives (10-4-19). The filter function for computing  $P(Z)^{n+1}$  from  $P(Z)^n$  is

$$\frac{(1 - aT) - Z(1 + aT)}{(1 + aT) - Z(1 - aT)} \quad (10-4-21)$$

We note that for positive  $a$  and for all  $T$  between 0 and 4, the denominator is a minimum-phase polynomial. This means that the time recurrence implied by (10-4-19) will be stable. The fact that (10-4-21) takes the form of an all-pass filter means that the depth recurrence on  $n$  will also be stable.

We have just completed a rather laborious stability proof. The reader will undoubtedly discover that his own application involves a slightly different equation, perhaps  $v = v(x, z)$  or increased angular accuracy. What general advice can be given about formulating problems so that they will be stable for extrapolation? To begin with, it helps if you have a physical feeling that all of the information must be flowing one way. Then, if trouble occurs, it is most likely to be at unsuspected values of  $\omega$ ,  $k_x$ ,  $k_z$ , or ratios thereof. Note that (10-4-15) in Fourier transform domain is

$$\omega k_z = -\frac{v}{2} k_x^2 \quad (10-4-22)$$

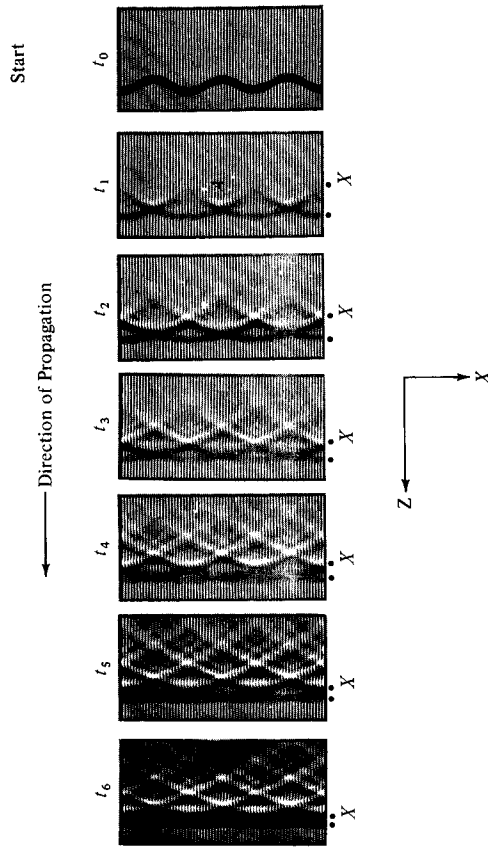


FIGURE 10-22

Disturbed plane wave propagating through a homogeneous medium. The first arrival of a disturbed plane wave heals itself during propagation. The wave coda or trail gets more and more complicated and energetic. In the trail, energy moves back away from the first arrival while phase fronts (marked by  $X$ ) move forward. Beam-steer signal processing (sum over the  $x$  coordinate) enhances the first arriving signal but tries to destroy later arriving signals (the trail). Although this calculation was done beginning with frame  $t_0$  and ending with frame  $t_6$ , the calculation could be done backwards, starting with  $t_6$  and ending with  $t_0$ . After time realignment, beam-steer on frame  $t_0$  could collect all signal energy.

If we are intending to extrapolate in the  $z$  direction we will be forming essentially  $\exp(ik_z z)$  or  $\exp(-ik_x^2 z^2 / \omega)$ . The reader should recall all the important facts about all-pass filters and spectral factorization. When wave propagation is to be modeled by all-pass filters and if the all-pass filters are supposed to be realizable or causal, then the phase derivative or group delay should be positive for all frequencies. We have in this case for the phase derivative

$$\frac{d}{d\omega}(k_z z) = -z \frac{v}{2} k_x^2 \frac{d}{d\omega} \left( \frac{1}{\omega} \right) = z \frac{v k_x^2}{2 \omega^2} \quad (10-4-23)$$

which is, as required, positive for all  $\omega$ . The fact that it is positive for all  $\omega$  and all  $k_x$  is important. Merely to be positive for values of  $\omega$  and  $k_x$  of practical interest is not enough. If for any value of  $\omega$  or  $k_x$  the group delay were negative, then the time domain extrapolation equations would blow up.

Finally, let us consider the example depicted in Fig. 10-22. In the first frame, a planar wavefront is deformed, as if by propagation through a region of velocity which varies periodically in the  $x$  direction. In optical terminology, the first frame of Fig. 10-22 would represent an impulsive plane wave just after emergence from a phase grating. In terms of atmospheric acoustics, the disturbance might arise from passage of a plane wave through the periodic circulation cells depicted in

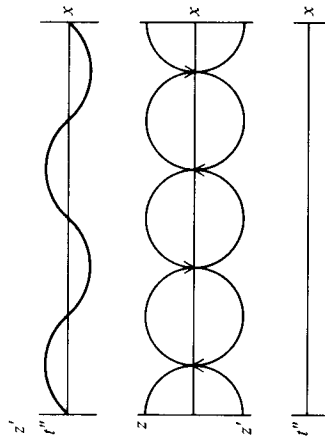


FIGURE 10-23  
Possible means of producing a disturbed plane wave. Incident plane wave at bottom is altered by a material inhomogeneity. For example, circulating air cells (center), resulting in the disturbed wave at the top.

Fig. 10-23. Successive frames in Fig. 10-22 depict the subsequent history of the waveform. In optics texts (e.g., Goodman, Reference 35, p. 69) the monochromatic solution is usually obtained at infinity. The most obvious development is that the energy spreads out as one moves to successive frames. The single pulse of the top frame has become an extended oscillatory arrival by the last frame. As time goes on, less and less energy is in the first pulse and more and more is in the oscillatory tail. Another very notable feature is that after some long time the first arrivals tend to be aligned again so that disturbances in a wavefront may be said to heal themselves as time goes on. In contrast, the coda (wave tail) develops into a spatially incoherent wave. (This mimics the behavior of most geophysical wave observations.) We may note several other less apparent aspects to Fig. 10-22. Although energy moves back from the first arrival, a point of constant phase in the wave tail (indicated by  $X$ ) moves forward toward the wave onset. Also the dip, or apparent direction of propagation, tends to increase going down a frame. This represents the ray interpretation that late arrivals have taken longer ray paths. Also the  $\pi/2$  phase shift of a two-dimensional focus which causes doublets to form may be seen at  $A$  in the second frame.

In order to represent a disturbance of infinite extent in  $x$  on a finite computer grid, the problem was initialized with a periodic disturbance having zero slope at the side boundaries. Zero-slope boundary conditions are then equivalent to infinite periodic extension in  $x$ . A value of  $v \Delta t \Delta z / \Delta x^2 = \frac{1}{4}$  was chosen to give an appropriate variation in progressive frames with each frame in Fig. 10-22 representing five computational iterations. The solution may be rescaled in several ways because of the interdependence of  $v \Delta t$ ,  $\Delta x$ , and  $\Delta z$ .

It might be valuable to consider various data enhancement processes in the light of Fig. 10-22. In the process called "beam-steering," observations such as those in Fig. 10-22 would be summed over the  $x$  coordinate in an effort to enhance signal and reject noise. Clearly beam-steering will enhance the first arrival while rejecting random noise. It will also tend to cancel signal energy which resides in the oscillatory wave tails. If one is really interested in enhancing signal-to-noise ratio it would hardly seem desirable to use a processing scheme which cancels signal energy. As  $z'$  or  $t'$  is increased the situation becomes increasingly severe, since signal energy moves from the initial pulse toward the oscillatory wave tails. What

has often been regarded as "signal-generated-noise" may turn out to be signal in a potentially valuable form. One can indeed expect dramatic results if enhancement techniques are based on entire waveforms rather than only on the initial pulse.

## EXERCISES

- 1 State all the assumptions which must be made to specialize (10-4-7) to  $[v(z) - \bar{v}]P_z = P_t'$ .
- 2 Derive the analogous equation for the double-prime coordinates.
- 2 Find a difference scheme for the equation of Exercise 1 which extrapolates from  $z'$  to  $(z' + \Delta z)$ . Show that past time is required if  $\bar{v} > v$  and future time if  $\bar{v} < v$ .
- 3 Let a coordinate transformation be defined by

$$x' = x$$

$$z' = z$$

$$t' = t - \int_0^z v^{-1}(z) dz$$

Put the scalar wave equation into these coordinates.

- 4 Show that if the transformation velocity  $\bar{v}$  in (10-4-9a), (10-4-9b), and (10-4-9c) takes any value less than the  $v$  in the wave equation, then stable difference equations will result.
- 5 Consider the difference equation  $(1 + \delta_{xx}/12) \delta_x P = b \delta_{xx} P$ . For what value of  $b$  does it reduce to an explicit scheme? Is the time recurrence stable for that value of  $b$ ?

## 10-5 BEAM COUPLING

Much of our information about the interior of the earth arises from interfaces within the earth which convert downgoing waves to upgoing waves. In layered media a mathematically strict decomposition of disturbances into downgoing waves  $[\exp(ik_z z)]$  and upcoming waves  $[\exp(-ik_z z)]$  was possible, but at present no such decomposition has been developed for two- or three-dimensional inhomogeneity: What we have is a collection of ad hoc techniques whose rigorous justification depends on the absence of horizontally propagating or evanescent energy. As a practical matter, what we are really interested in is not just the decomposition of waves into downgoing and upgoing parts. We are interested in describing the interactions between more-or-less collimated beams. In holography, these are the *incident* (or reference) beam and the *scattered* beam. In global seismology, these could be the incident compressional wave beam and the scattered shear wave beam. They need not have any particular orientation to each other or to the vertical.

The wave-extrapolation techniques described earlier can be used to describe beams collimated roughly along the  $z$  axis. Now we take up the task of describing the interaction between two such beams. For simplicity, these will initially be taken to be two more-or-less vertically propagating beams, one going down, the



other up, interacting at a planar horizontal interface. The technique developed can then be applied to a great many less restrictive geometries. The accuracy of results in more general geometries is then a practical question whose answer varies from one situation to the next. Accuracy limitations come from many sources, which include

- 1 Angular dependence of velocity in the collimated beam which arises from Fresnel-like approximations
- 2 Neglect of evanescent energy
- 3 Possible inability of two collimated-beam equations to describe all important beams generated at a complicated interface
- 4 Approximation of elastic compressional waves by the scalar wave equation.

The significance of accuracy limitations must be evaluated in terms of accuracy of experimental work, required accuracy, and accuracy and cost of competitive techniques. Such evaluations are completely beyond the scope of our present efforts.

In this section we will describe only the *primary* reflected seismic energy in reflection seismic exploration. Large-amplitude waves are initiated at the earth's surface by means of dynamite or other high-energy sources. These waves penetrate into the earth where a small fraction of the energy echoes at weak reflectors and gets sent back to sensitive surface geophones. Occasional situations where a noticeable amount of energy scatters up and down several times (called multiple reflections or just multiples) will be discussed in a later section. For a plane layered medium we can use equation (9-3-13).

$$\frac{d}{dz} \begin{bmatrix} U \\ D \end{bmatrix} = \begin{bmatrix} -iab & \\ & iab \end{bmatrix} \begin{bmatrix} U \\ D \end{bmatrix} - \frac{1}{2} \frac{Y_z}{Y} \begin{bmatrix} 1 & -1 \\ -1 & 1 \end{bmatrix} \begin{bmatrix} U \\ D \end{bmatrix} \quad (10-5-1)$$

Because the practical situation which we are trying to describe satisfies the inequality  $U \ll D$ , we will approximate the lower equation in (10-5-1) by

$$D_z = iabD - \frac{Y_z}{2Y} D \quad (10-5-2)$$

To get a physical understanding of (10-5-2) which is applicable even when  $a$ ,  $b$ , and  $Y$  are  $z$ -variable, note that the solution to (10-5-2) which can be verified by direct substitution, is

$$D = D_0 Y^{-1/2} \exp \left( i \int_0^z ab \, dz \right) \quad (10-5-3)$$

In other words,  $iab$  controls the phase (or velocity) of the wave and  $Y_z/Y$  controls amplitude change. Thus, we can interpret the  $Y_z/Y$  term as providing the physical effect associated with a transmission coefficient. It often happens that the velocity information in  $ab$  is approximately known, but the location of interfaces in the earth given by discontinuities in  $Y_z/Y$  are totally unknown. This means that we

need not abandon our calculation of  $D$  if we are prepared to admit that its amplitude errs by the unknown transmission coefficients.

The basic thrust of Sec. 10-3 was that we can treat nonplanar waves by regarding  $iab$  as the square root of the differential operator  $-(\omega^2/v^2 + \partial_{xx})$ . For a beam collimated downward along the  $z$  axis a first approximation to the square root is given by  $i\omega/v[1 + v^2(\partial_{xx}/2\omega^2)]$ . With the beam-collimation assumption ( $\partial_{zz} \approx 0$ ) and the unknown admittance gradient taken as zero, the downgoing wave  $D$  can be calculated with the equation

$$D_z = \frac{i\omega}{v} D + \frac{iv}{2\omega} D_{xx} \quad (10-5-4)$$

This would more closely resemble the bulk of our earlier work if we assumed homogeneous velocity  $v = \bar{v}$  and then made the transformation  $D = D'e^{imz}$  where  $m = \omega/v$ , in which case (10-5-4) would reduce to

$$D'_z = \frac{iv}{2\omega} D'_{xx} \quad (10-5-5)$$

To solve (10-5-4) or (10-5-5) inside the earth it is only necessary to know values for  $D$  along the surface of the earth (all  $x$ ,  $z = 0$ ). In a reflection seismic prospecting situation,  $D$  could usually be approximated by a delta function at the shot location.

Now let us turn to the calculation of the upgoing wave  $U$ . From the top row of (10-5-1) we have

$$U_z = -iabU - \frac{Y_z}{2Y}(U - D) \quad (10-5-6)$$

If we care to neglect the transmission coefficient effect on  $U$  while retaining the reflection coefficient interaction of  $U$  and  $D$ , this becomes

$$U_z = -iabU + \frac{Y_z}{2Y} D \quad (10-5-7)$$

Because reflection coefficient  $c$  is defined as

$$c = \frac{Y_2 - Y_1}{Y_2 + Y_1} = -c'$$

we can [for  $Y(z)$  differentiable] write (10-5-7) as

$$U_z = -iabU - c'(z)D \quad (10-5-8)$$

As with the downgoing waves, we can generalize from plane waves to beams with the square root approximation, obtaining

$$U_z = -\frac{i\omega}{v} U - \frac{iv}{2\omega} U_{xx} - c'(x, z)D \quad (10-5-9)$$

A change of variables to  $U = U''e^{-imz}$  and  $D = D'e^{imz}$  with the homogeneous velocity, inhomogeneous-admittance assumption converts (10-5-9) to

$$U''_z = -\frac{\bar{v}/2}{-i\omega} U''_{xx} - c'(x, z)D'e^{2imz} \quad (10-5-10)$$

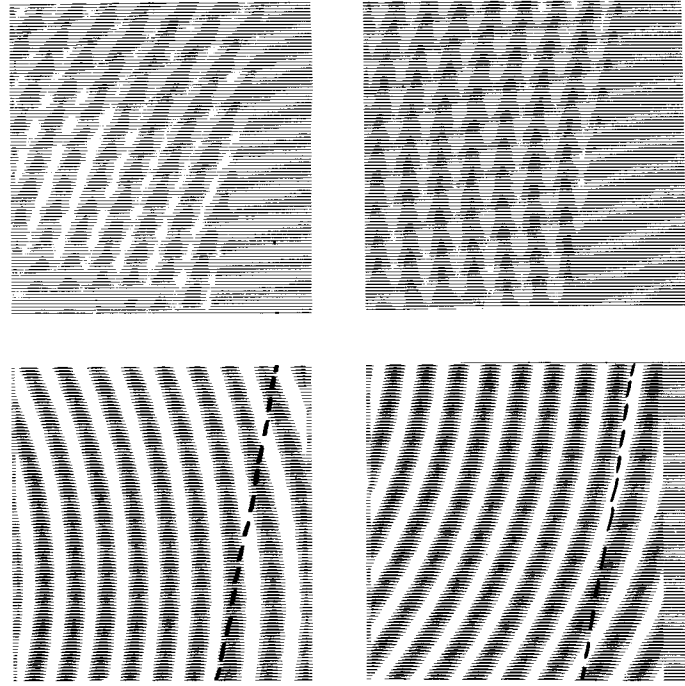


FIGURE 10-24

Two examples of down- and upgoing waves. The two left-hand frames show downgoing spherical waves from two different source locations. These waves illuminate a dipping interface. At the interface is both an impedance contrast and a velocity contrast. Waves of longer wavelength are seen below the interface. The right-hand frames show the upcoming waves. They vanish beneath the interface. Along the interface, the phase of the upcoming wave equals that of the downgoing wave.

It is important to understand how we can calculate the solution to (10-5-10). First of all,  $D'$  must have been calculated by some other equation before we start on  $U''$ . In the solution of (10-5-10) we will regard  $c(x, z)D'$  as a source term for the generation of  $U''$ . Now there are two important cases. The first one is data synthesis. This is called the *forward* problem. The other case, called the *inverse* problem, is where the data sample  $U''$  is given at the earth's surface,  $z = 0$ , and the problem is to deduce both  $c(z)$  and  $U''(z)$  as you integrate  $U''$  downward. The inverse problem is more fully treated in the chapter on seismic data processing. Here we will stick to the forward problem. A boundary condition on  $U''$  which will enable us to use (10-5-9) to find  $U''$  everywhere is to prescribe that  $U''$  vanishes over all  $x$  inside the earth at some depth  $z_N$  which is suitably great, say beneath all detectable reflectors. Then (10-5-10) is stepped up from  $z_N$  to  $z_{N-1}$ ,  $z_{N-2}$ , etc.  $U''$  remains zero until we come up to the first illuminated reflector; that is, the deepest place where both  $c(x, z)$  and  $D'$  are nonvanishing. At this point, the source term in

(10-5-10) is turned on and  $U''$  becomes nonzero from then on upward. This calculation is illustrated in Fig. 10-24.

The calculation can also be done in the time domain. We have the downgoing wave transformation

$$x' = x \quad (10-5-11a)$$

$$z' = z \quad (10-5-11b)$$

$$t' = t - \frac{z}{\bar{v}} \quad (10-5-11c)$$

and the upgoing wave transformation

$$x'' = x \quad (10-5-12a)$$

$$z'' = z \quad (10-5-12b)$$

$$t'' = t + \frac{z}{\bar{v}} \quad (10-5-12c)$$

And we have the possibility of expressing  $U$  and  $D$  in either frames (10-5-11) or frames (10-5-12)

$$U(x, z, t) = U'(x', z', t') = U''(x'', z'', t'') \quad (10-5-13a)$$

$$D(x, z, t) = D'(x', z', t') = D''(x'', z'', t'') \quad (10-5-13b)$$

The chain rule for differentiation gives

$$\partial_x D = \partial_x D' \quad (10-5-14a)$$

$$\partial_z D = \left( \partial_z - \frac{1}{\bar{v}} \partial_t \right) D' \quad (10-5-14b)$$

$$\partial_t D = \partial_t D' = \partial_t D'' \quad (10-5-14c)$$

and

$$\partial_x U = \partial_x U' \quad (10-5-15a)$$

$$\partial_z U = \left( \partial_z + \frac{1}{\bar{v}} \partial_t \right) U' \quad (10-5-15b)$$

$$\partial_t U = \partial_t U' \quad (10-5-15c)$$

Taking velocity-homogeneous media  $v = \bar{v}$ , multiplying (10-5-4) and (10-5-9) through by  $-i\omega$ , and then identifying  $-i\omega$  with a time derivative, we obtain

$$D_{zt} = -\frac{1}{\bar{v}} D_{tz} + \frac{\bar{v}}{2} D_{xx} \quad (10-5-16a)$$

$$U_{zt} = \frac{1}{\bar{v}} U_{tz} - \frac{\bar{v}}{2} U_{xx} - c'(x, z)D_t \quad (10-5-16b)$$

Equations (10-5-16a) and (10-5-16b) are readily converted by means of (10-5-14) and (10-5-15) to

$$D'_{z't'} = \frac{\bar{v}}{2} D'_{x'x'} \quad (10-5-17a)$$

$$U''_{z't'} = -\frac{\bar{v}}{2} U''_{x'x'} - c'(x'', z'') D''_{t'} \quad (10-5-17b)$$

Now (10-5-17a) can be used to compute  $D'$  but (10-5-17b) calls for  $D''$ . Subtracting (10-5-12c) from (10-5-11c) we get

$$t' = t'' - \frac{2z}{\bar{v}}$$

So, using (10-5-13b) we find (10-5-17b) can be expressed in terms of  $D'$  as

$$U''_{z't'} = -\frac{\bar{v}}{2} U''_{x'x'} - c'(x'', z'') \partial_{t'} D' \left( x'', z'', t'' - \frac{2z''}{\bar{v}} \right) \quad (10-5-18)$$

This time-domain result is the transform of (10-5-10).

## EXERCISES

- 1 Show that  $\frac{1}{2}[(d/dz) \ln |J|]$  is the reflection coefficient  $c'$  as seen from above the interface.
- 2 Recall from (9-3-20) that the definition of  $Y$  includes  $k_x$ . This was neglected in the derivation of (10-5-10). Improve (10-5-10) to include the implied  $\partial D'/\partial x$  terms. This improvement allows reflection coefficient to be a function of angle.

## 10-6 NUMERICAL VISCOSITY

Positive numerical viscosity means that the short wavelength deviation of a difference equation from a differential equation is such that the short wavelengths tend to dissipate as the calculation proceeds. The numerical viscosity may also turn out to be negative, causing short wavelengths to amplify rather than attenuate. Whether or not there are good scientific reasons to study numerical viscosity, scientists often get dragged into this study for several reasons: First, even if differential equations do not violate causality there may be instability due to negative viscosity in the difference equations. Second, the realities of computer economics (especially in a multidimensional problem such as  $P_{z,t} = (v/2)P_{xx}$  may require that waveforms be sampled with as few points as practicable. Third, when observational data are to be processed, as when  $P(x, t)$  is to be extrapolated from  $z_1$  to  $z_2$ , then the data may be inconsistent with certain assumptions upon which the extrapolating equation is based.

For example, suppose that  $P(x, t)$  has Fourier transform  $P'(k_x, \omega)$ . Then, since  $k_x^2 + k_z^2 = \omega^2/v^2$ , freely propagating waves are characterized by  $|k_x| < \omega/v$

Points per wavelength, $2\pi/\omega \Delta t$	$\omega \Delta t$ or $k_x \Delta x$ , radians	Relative error of $2 \tan \omega \Delta t/2$	Relative error of $2 \sin k_x \Delta x/2$	Relative error of (10-6-8)
$\pi \times 10^n$	$2 \times 10^{-n}$	$10^{-2n/3}$	$10^{-2n/6}$	$0(10^{-4n})$
20.000000	0.314159	0.008272	-0.004116	-0.000021
16.000000	0.392699	0.012968	-0.006434	-0.000051
12.000000	0.523599	0.023218	-0.011449	-0.000159
10.000000	0.628318	0.033675	-0.016504	-0.000330
8.000000	0.785398	0.053325	-0.025834	-0.000812
6.000000	1.047197	0.097645	-0.046109	-0.002613
4.000000	1.570796	0.240396	-0.104913	-0.013849
3.000000	2.094395	0.492833	-0.189390	-0.046111
2.100000	2.991992	1.596763	-0.400123	-0.203548

FIGURE 10-25

The relative error at short wavelengths often associated with expressing differential equations in difference form.

so  $P'(k_x, \omega)$  should vanish unless  $|k_x| < \omega/v$ . In the derivation of  $P_{z,t} = v/2 P_{xx}$  it was further assumed that the waves have small angles of propagation; hence, the inequality becomes stronger,  $|k_x| \ll \omega/v$ . Since observational data will certainly not satisfy these conditions exactly we have two options. First, we can hope to ignore the illegal part of the  $(k_x, \omega)$  space if the data do not have much energy there and if our difference equation does not unacceptably amplify it. Second, we can modify our difference or differential equations so that there is a controlled positive numerical viscosity in the illegal part of the transform space. This kind of operation is sometimes called fan-filtering because of the wedge-shaped region of attenuation in  $(\omega, k_x)$  space.

The operator  $\partial_{xx}$  has the Fourier transform  $-k_x^2$ . The operator  $\delta_{xx}$  amounts to a convolution on the  $x$  axis with the coefficients  $(1, -2, 1)/\Delta x^2$ , thus its Fourier transform is  $[\exp(-ik_x \Delta x) - 2 + \exp(ik_x \Delta x)]/\Delta x^2$ . We write this as

$$FT(\partial_{xx}) = -k_x^2 \quad (10-6-1a)$$

$$FT\left(\frac{\delta_{xx}}{\Delta x^2}\right) = -\hat{k}_x^2$$

$$= -\frac{2(1 - \cos k_x \Delta x)}{\Delta x^2}$$

$$FT\left(\frac{\delta_{xx}}{\Delta x^2}\right) = -\frac{2^2}{\Delta x^2} \sin^2\left(\frac{k_x \Delta x}{2}\right) \quad (10-6-1b)$$

The approximation  $\hat{k}_x$  to  $k_x$  is given by

$$\hat{k}_x = \frac{2}{\Delta x} \sin k_x \frac{\Delta x}{2} \quad (10-6-2)$$

The error in the approximation  $\hat{k}_x \approx k_x$  is tabulated in Fig. 10-25.

The Crank-Nicolson method amounts to another approximation. Here the operator  $\partial/\partial t$  which has the Fourier transform  $-i\omega$  is approximated by the bilinear transformation. The approximation  $\hat{\omega}$  to  $\omega$  is given by

$$-i\hat{\omega} \Delta t = \frac{2(1 - e^{i\omega \Delta t})}{1 + e^{i\omega \Delta t}}$$

Multiplying top and bottom on the right by  $e^{-i\omega \Delta t/2}$  we get

$$\begin{aligned} -i\hat{\omega} \Delta t &= 2 \frac{e^{-i\omega \Delta t/2} - e^{i\omega \Delta t/2}}{e^{-i\omega \Delta t/2} + e^{i\omega \Delta t/2}} \\ &= -2i \tan \frac{\omega \Delta t}{2} \end{aligned} \quad (10-6-3)$$

$$\hat{\omega} = \frac{2}{\Delta t} \tan \frac{\omega \Delta t}{2}$$

This approximation is also tabulated in Fig. 10-25.

To see how higher-order difference approximations may be built up, we solve (10-6-2) for  $ik_x$  getting

$$ik_x = \frac{2}{\Delta x} \operatorname{arcsinh} \left( \frac{ik_x \Delta x}{2} \right) \quad (10-6-4)$$

Recall the power series for  $\operatorname{arcsinh}$

$$\operatorname{arcsinh} u = u - \frac{1}{2} \frac{u^3}{3} + \frac{1}{4} \frac{u^5}{5} - \frac{1}{8} \frac{u^7}{7} + \dots \quad (10-6-5)$$

The inverse Fourier transform of (10-6-4) using (10-6-5) provides a power series expansion for  $\hat{\omega}_x$  in terms of powers of  $\delta_x$ .

At the present time, reflection seismic data often come close to being under-sampled in the horizontal  $x$  coordinate. Hence, it is worthwhile to devise a more accurate approximation than  $\delta_{xx}$  to  $\hat{\omega}_{xx}$ . Squaring (10-6-4) and retaining only the first two terms in the  $\operatorname{arcsinh}$  expansion gives

$$-k_x^2 \approx \frac{4}{\Delta x^2} \left( u^2 - \frac{u^4}{3} \right) \quad (10-6-6)$$

where  $u = ik_x \Delta x/2$ . Taking the inverse transform we have

$$\hat{\omega}_{xx} \approx \frac{\delta_{xx}(1 - \delta_{xx}/12)}{\Delta x^2} \quad (10-6-7)$$

It is most often convenient to use this in the rational form

$$\hat{\omega}_{xx} \approx \frac{\delta_{xx}/\Delta x^2}{1 + \delta_{xx}/12} \quad (10-6-8)$$

By means of a trick, the rational form can be used without going to higher-order difference operators. Note that (10-6-8) into a differential equation of the type  $P_t = P_{xx}$  leads to

$$\left( 1 + \frac{\delta_{xx}}{12} \right) \delta_t P = \frac{\Delta t}{\Delta x^2} \delta_{xx} P \quad (10-6-9)$$

The new term  $\delta_{xx} P$  fits on the old computation star and thus amounts to a just readjustment of coefficients; that is, hardly any increase in computer costs. Reference to Fig. 10-25 shows an astonishing increase in accuracy. On the basis of Fig. 10-25 and the acceptable error for some particular application, say 3 per cent, one determines a minimum acceptable number of points per wavelength, say 10 points per wavelength on  $z$  and  $t$  axes and  $3\frac{1}{2}$  points per wavelength on the  $x$  axis. Then the useful bandwidth  $-2\pi/10 < \omega \Delta t < +2\pi/10$  is markedly less than the total bandwidth available ( $2\pi$  is the periodicity interval for transforms of sampled data). In this case, the ratio of useful bandwidth to total bandwidth is  $1/5$ . In order to use more of the available bandwidth it is necessary to put up with more error or to develop more elaborate difference approximations to differential operators. Figure 10-26 depicts the paltry portion of  $(\omega, k_x)$  space which is usable.

For examples of the manipulation of numerical viscosity let us take the differential equation  $P_{zt} = v/2 P_{xx}$  and modify it to attenuate energy outside the usable bandwidth, say where  $|k_x \Delta x| > \pi/5$ . We simply add a term to the right-hand side. That is, we modify

$$\hat{\omega}_z P = \frac{v}{-2i\omega} \hat{\omega}_{xx} P \quad (10-6-10)$$

by judicious choice of an additional term

$$\hat{\omega}_z P = \frac{v}{-2i\omega} \hat{\omega}_{xx} P + a \hat{\omega}_{xx} P \quad (10-6-11)$$

To see what numerical value to take for the constant  $a$ , we transform the  $x$  coordinate in (10-6-11)

$$\hat{\omega}_z P = \left( \frac{vk_x^2}{2i\omega} - ak_x^2 \right) P \quad (10-6-12)$$

Equation (10-6-12) has the solution

$$P(z) = P(z_0) \exp \left[ \left( \frac{vk_x^2}{2i\omega} - ak_x^2 \right) (z - z_0) \right] \quad (10-6-13)$$

The imaginary part of the exponent merely gives the phase angle, which we will ignore because we are interested only in magnitude. Let  $z - z_0 = d$ . Then (10-6-13) becomes

$$\left| \frac{P(z)}{P(z_0)} \right| = \exp(-ak_x^2 d) \quad (10-6-14)$$

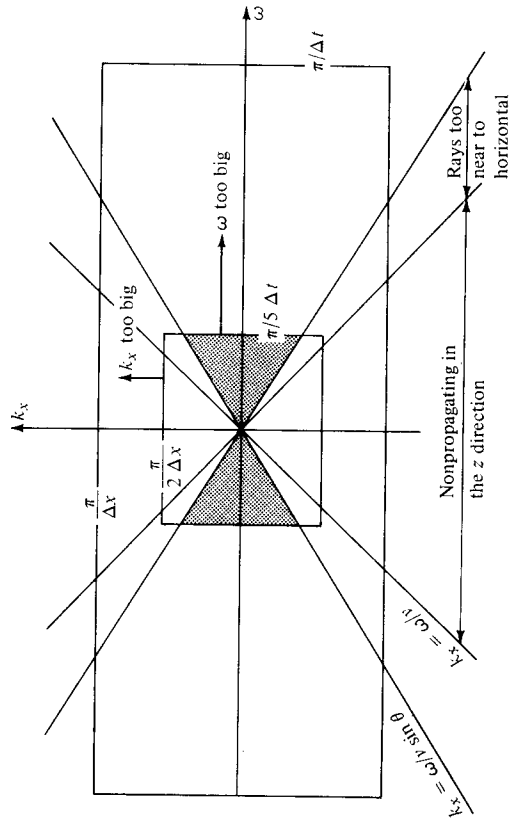


FIGURE 10-26 The  $(\omega, k_x)$  plane. Field data may be expected to have some energy everywhere in the  $(\omega, k_x)$  plane. Only in the speckled region will our difference equations properly simulate the wave equation. Energy with  $|k_x| > |\omega/v|$  does not represent free waves; it represents either surface waves or errors in data collection (often static errors, random noise, or gain not smoothly variable from trace to trace). Such energy can mean nothing in a migration program, hence it should be rejected by filtering. This may be done by fan-filtering (as in Reference 36) or, as is done here, by means of numerical viscosity. Actually, for practical reasons one frequently may wish to reject rays outside a certain dip angle. This gives the larger fan-filter reject region  $|k_x| > |\omega/v \sin(\text{dip})|$ . Although information can be carried up to the folding frequency in both  $\omega$  and  $k_x$ , in practice the use of operators of finite length narrows the useful bandwidth. The use of simple time-difference operators results in a practical bandwidth restriction to about a quarter of the folding frequency. This presents no problem in principle; data may be interpolated before processing, or more elaborate (i.e., longer) difference operators may be used.

Now we have to decide how much attenuation is wanted. Say when  $k_x \Delta x = \pi/4$  we wish (10-6-14) to imply attenuation to  $e^{-1}$ . Thus, for the exponential of (10-6-14), we have

$$\begin{aligned}
 -ak_x^2 d &= -1 \\
 a(k_x \Delta x)^2 \frac{d}{\Delta x^2} &= 1 \\
 a \left(\frac{\pi}{4}\right)^2 \frac{d}{\Delta x^2} &= 1 \\
 a &= \frac{16 \Delta x^2}{d\pi^2} \quad (10-6-15)
 \end{aligned}$$

Thus, the term we added to (10-6-10) to get (10-6-11) has a coefficient which goes to 0 as the squared grid spacing  $\Delta x^2$ . Inclusion of this term gives the gaussian attenuation function of spatial frequency of (10-6-14). The inclusion of the viscosity term seems to add virtually no cost to a computer program.

Next, let us modify the extrapolation equation so that excessive dips  $[\sin(\text{dip}) = kv/\omega]$  will be attenuated. This is not exactly numerical viscosity because we will alter the basic differential equation. It is like numerical viscosity in that it is an ad hoc modification intended to correct a certain deficiency. Here we modify the differential equation (10-6-10) to read

$$\partial_z P = \frac{v \partial_{xx}}{2(-i\omega + \omega_0)} P \quad (10-6-16)$$

To see what numerical value to pick for  $\omega_0$ , we rationalize the denominator

$$\partial_z P = \frac{v}{2} \frac{i\omega + \omega_0}{(\omega^2 + \omega_0^2)} \partial_{xx} P \quad (10-6-17)$$

Now we may ignore the imaginary part of the right-hand side of (10-6-17) because it contributes only the phase of  $P$ . Fourier transforming the  $x$  coordinate, we have

$$\partial_z P = -\frac{v \omega_0 k_x^2}{2(\omega^2 + \omega_0^2)} P \quad (10-6-18)$$

There are two cases. We will pick  $\omega_0$  very small so that in the uninteresting case where  $\omega < \omega_0$  (10-6-18) reduces to spatial frequency dissipation but in the interesting case  $\omega > \omega_0$  (10-6-18) amounts to

$$\partial_z P = -\frac{v \omega_0 k_x^2}{2 \omega^2} P \quad (10-6-19)$$

This is obviously attenuation, which is a gaussian function of dip. It is left for the exercises to find a numerical choice for  $\omega_0$ .

EXERCISES

- 1 What value of  $\omega_0$  in (10-6-16) will attenuate waves propagating from  $z_1$  to  $z_2$  at a  $30^\circ$  angle from the  $z$  axis to  $e^{-1}$  times the original amplitude? So that  $\omega_0$  may be said to be small, it is necessary to compare it to something with physical dimensions of inverse time. Give examples of a situation where  $\omega_0$  is small and a situation where it is not.
- 2 Show that the parameter  $b$  in  $P_z = iv/2\omega(\partial_{xx} + b \partial_{xxz})P$  may be used to produce a viscosity decay of approximate form  $\exp[-bk_x^2(z - z_0)]$ . This may be useful when  $\Delta z$  is taken too large.
- 3 Consider extrapolation one step in the  $z$  direction with the equation  $P_z = -a\omega^2 P$ . Insert the bilinear transformation  $-i\omega = 2(1 - Z)/(1 + Z)$  and deduce that the equation cannot be used since a polynomial with a nonminimum-phase divisor results.

## SEISMIC DATA PROCESSING WITH THE WAVE EQUATION

- 4 Show that the equation  $P_z = a(-\omega^2 \Delta t^2 / 2 + i\omega \Delta t)P$ , unlike the equation of Exercise 3, leads to a causal time-domain filter. (Do the extrapolation in  $z$  by the Crank-Nicolson method, i.e., the bilinear transform method.)
- 5 A given set of data  $P(x, t)$  is believed to satisfy the equation  $P_{zt} = P_{xx}$ . It is observed that transformed data  $Q(x, t) = P(x, t)e^{\alpha t}$ , fits into a reasonably small numerical range so that  $Q$  may be represented using integer arithmetic. What differential equation does  $Q$  satisfy?

The coordinate frames used by theoreticians to describe wave propagation do not include frames in common use by geophysical prospectors to describe observations. Whereas the theoretician generally considers a single source (or shot) location at a time, the experimentalist deals simultaneously with waves which have been generated separately by many shots. Our task in this section is to put the wave equation into some prospectors' coordinate frames.

### 11-1 DOWNWARD CONTINUATION OF GATHERS AND SECTIONS

Suboceanic prospecting is generally carried out by a ship which carries a repetitive energy source and which trails a cable that is 2 to 3 kilometers long and packed with sonic receivers. Ideally, the ship's course is a straight line which we can take to be the  $x$  axis. Ideally, all the seismic waves of interest propagate in a vertical plane through the line of the ship's course. This plane is called the plane of the seismic section. Despite the fact that it is no great problem to describe waves in